

# THE AKHIEZER ITERATION AND AN INVERSE-FREE SOLVER FOR SYLVESTER MATRIX EQUATIONS

CADE BALLEW, THOMAS TROGDON, AND HEATHER WILBER

**ABSTRACT.** An inverse-free iterative method is developed for solving Sylvester matrix equations when the spectra of the coefficient matrices are on, or near, known disjoint subintervals of the real axis. The method uses the recently-introduced Akhiezer iteration to address an equivalent problem of approximating the matrix sign function applied to a block matrix, resulting in a provable and computable geometric rate of convergence. When the right-hand side matrix is low rank, the method requires only low-rank matrix-matrix products. Relative to existing state-of-the-art approaches, the method presented here can be more efficient when the coefficient matrices are dense or otherwise costly to invert. Applications include solving partial differential equations and computing Fréchet derivatives.

## 1. INTRODUCTION

In numerical linear algebra, a fundamental problem is computing the solution of the Sylvester matrix equation, which is given by

$$(1) \quad \mathbf{X}\mathbf{A} - \mathbf{B}\mathbf{X} = \mathbf{C}, \quad \mathbf{X}, \mathbf{C} \in \mathbb{C}^{m \times n}, \quad \mathbf{A} \in \mathbb{C}^{n \times n}, \quad \mathbf{B} \in \mathbb{C}^{m \times m},$$

with  $\mathbf{X}$  as the unknown. It appears in applications related to model reduction and stability analysis for large-scale dynamical systems [3, 30, 48], eigenvalue assignment for vibrating structures [20], noise reduction in image processing [21], various tasks in control systems and signal processing [13, 26, 36, 60], and the solving of partial differential equations (PDEs) [19, 25, 40, 54]. We consider the case where the *coefficient matrices*  $\mathbf{A}$  and  $\mathbf{B}$  are diagonalizable with spectra each contained in disjoint regions on or near the real axis.

Iterative methods for solving these equations have been a central focus of research for several decades (see [53] and the references therein), and this has co-evolved alongside the broader development of rational Krylov methods [11, 17, 50] and related iterative solvers that fundamentally involve approximations via rational functions. In settings where  $\mathbf{C}$  is low rank and  $\mathbf{A}$  and  $\mathbf{B}$  are banded, sparse, or otherwise structured so that shifted inverses are inexpensive, rational-based iterative methods can be extraordinarily effective. However, when  $\mathbf{A}$  and  $\mathbf{B}$  are dense or otherwise costly to invert, such methods will become prohibitively expensive, offering no advantage over the  $O(m^3 + n^3)$  direct solver of Bartels and Stewart [9], which is itself too costly in the large scale setting. A natural alternative one might look for is an iterative method based on polynomial approximation. This would avoid the costs of inversion, instead requiring low-rank matrix-matrix products when  $\mathbf{C}$  is low rank. Unfortunately, existing methods based on such ideas (e.g., polynomial Krylov methods) tend to converge slowly enough in most settings that they are practically ineffective [52].

Here, we introduce a new polynomial-based iterative method for solving Sylvester matrix equations. Unlike other polynomial-based methods, ours relies on the use of so-called *Akhiezer polynomials* [1, Chapter 10], a generalization of the Chebyshev polynomials that are orthogonal with respect to a weighted inner product over domains consisting of disjoint intervals on the real axis. Because these polynomials have good convergence properties on cut domains, we are able to obtain rates of convergence in our algorithms that are geometric with the degree of the polynomial (and number of iterations). The result is a collection of inverse-free iterative methods with convergence properties closer to those of rational-based methods (see Figure 1). When  $\mathbf{C}$  is low rank, as is

often the case in practice, our methods only require low-rank matrix-matrix products and some low-dimensional QR and singular value decompositions. When  $\mathbf{X}$  is numerically of low rank, our method can be used to construct an approximate solution in low-rank form.

**1.1. An approach based on the matrix sign function.** The two primary classes of iterative methods developed for solving (1) are those based on Krylov subspace projections, such as the extended Krylov method [52] and the rational Krylov subspace method [10, 24], and those based around directly using rational approximations to construct low-rank solutions, including the cyclic Smith method [48, 51, 55], the low-rank alternating direction implicit (LR-ADI) method [14, 37], and their variants. A distinct idea, first introduced by Roberts in [49] in the context of solving matrix Riccati equations, is based instead on approximating the matrix sign function [16, 23, 31]. This is also the core idea animating our method. We define the sign function somewhat unconventionally as follows:

**Definition 1.1.** *Let  $U_{\mathbf{A}}$  and  $U_{\mathbf{B}}$  denote two disjoint sets in  $\mathbb{C}$ . Then, the function  $\text{sign}(z) = \text{sign}(z; U_{\mathbf{A}}, U_{\mathbf{B}})$  is defined on  $U_{\mathbf{A}} \cup U_{\mathbf{B}}$  as*

$$\text{sign}(z) = \begin{cases} 1, & z \in U_{\mathbf{A}}, \\ -1, & z \in U_{\mathbf{B}}. \end{cases}$$

When the context is clear, we simplify the notation and simply refer to  $\text{sign}(z)$  without explicitly listing the sets it is defined on. We also use  $\sigma(\mathbf{M})$  to denote the set of eigenvalues of a square matrix  $\mathbf{M}$ , i.e., the spectrum. If  $\sigma(\mathbf{A}) \subset U_{\mathbf{A}}$  and  $\sigma(\mathbf{B}) \subset U_{\mathbf{B}}$ , then using the definitions for matrix functions we develop below,

$$(2) \quad \text{sign} \underbrace{\begin{pmatrix} \mathbf{A} & \mathbf{0} \\ \mathbf{C} & \mathbf{B} \end{pmatrix}}_{\mathbf{H}} = \begin{pmatrix} \mathbf{I}_n & \mathbf{0} \\ \mathbf{X} & \mathbf{I}_m \end{pmatrix} \begin{pmatrix} \mathbf{I}_n & \mathbf{0} \\ \mathbf{0} & -\mathbf{I}_m \end{pmatrix} \begin{pmatrix} \mathbf{I}_n & \mathbf{0} \\ -\mathbf{X} & \mathbf{I}_m \end{pmatrix} = \begin{pmatrix} \mathbf{I}_n & \mathbf{0} \\ 2\mathbf{X} & -\mathbf{I}_m \end{pmatrix}.$$

Using (2), the solution  $\mathbf{X}$  of (1) can be obtained by computing the matrix  $\frac{1}{2} \text{sign}(\mathbf{H})$  and isolating the lower left block [31, Section 2.4]. To get an inverse-free iterative method for computing  $\mathbf{X}$  from this, we construct an approximation

$$(3) \quad \text{sign}(z) \approx \sum_{j=1}^m \alpha_j p_j(z),$$

where  $(p_j(z))_{j=0}^{\infty}$  are the Akhiezer polynomials, and are therefore orthogonal with respect to a special inner product. An efficient numerical method for evaluating these polynomials (and computing the coefficients  $\alpha_j$  in the expansion) was recently introduced in [5, 6]. In principle, one can simply evaluate (3) at  $z = \mathbf{H}$  and extract the appropriate block to create an approximate solution to (1). Evaluating each  $p_j(\mathbf{H})$  directly is expensive since the dimensions of  $\mathbf{H}$  are double those of the original problem, and we seek to avoid this. Using the block triangular structure and the three-term recurrence satisfied by the Akhiezer polynomials, we develop a recursion that describes the evolution of the lower left block as  $j$  grows, so that our method only incurs a computational cost that is linear with respect to the cost of matrix-vector products with  $\mathbf{A}$  and  $\mathbf{B}$ . Under our convergence heuristics,  $O(\log(m+n))$  iterations are required to satisfy an error tolerance, and therefore the overall cost of the low-rank variation of the method when  $\mathbf{A}$  and  $\mathbf{B}$  are dense is  $O(m^2 \log m + n^2 \log n)$ . Furthermore, as we demonstrate in Figure 7, our method often has a shorter runtime than competing methods, even for small problems.

Inverse-free iterative solvers can be advantageous in settings where the coefficient matrices are dense, where fast matrix-vector product routines for these matrices are available, and in settings where coefficient matrices are not directly accessible and only their action can be observed. Outside recent developments in [46] where the slower convergence of a polynomial-based method is paired with sketching to greatly reduce the per-iteration cost, polynomial methods for such problems have

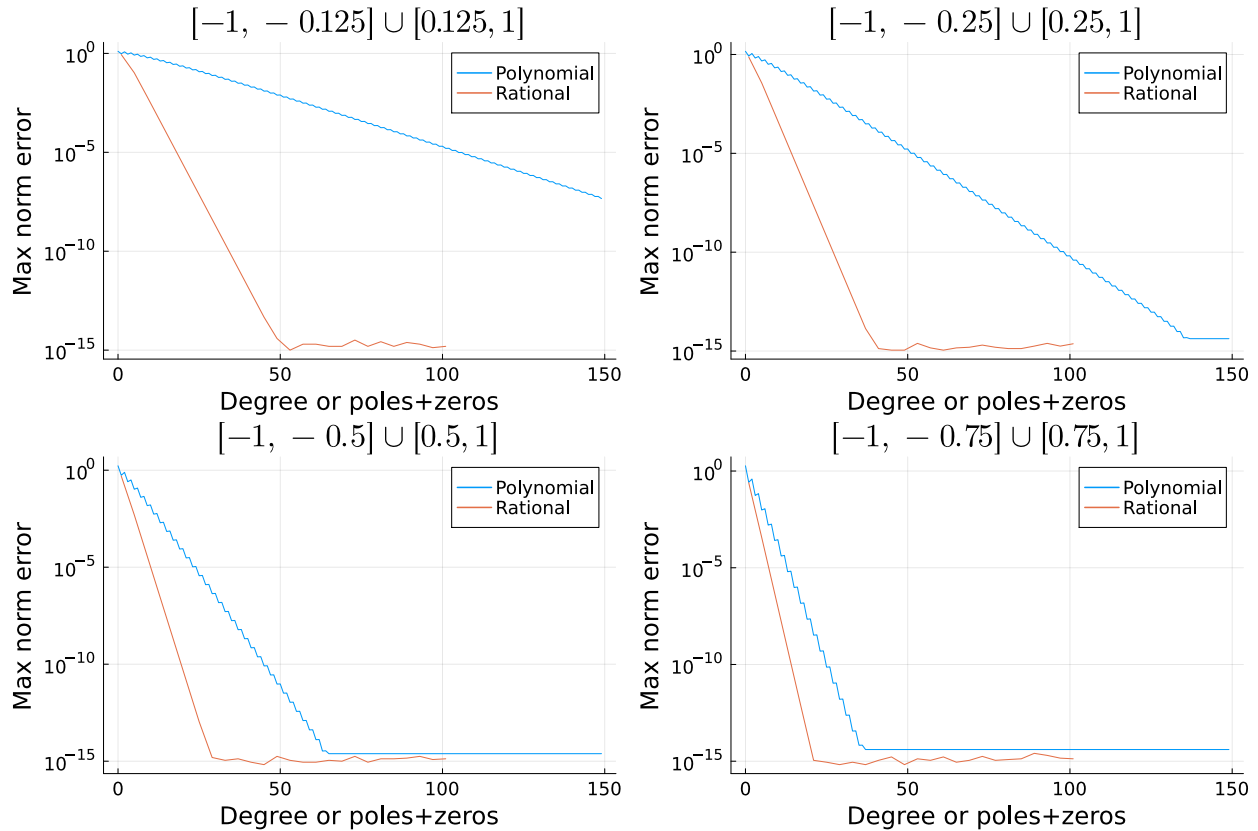


FIGURE 1. Error plots of Akhiezer polynomial and optimal Zolotarev rational approximations to the sign function on different cut domains.

not been widely explored. Our hope is that the new availability of a fast inverse-free method will prompt further developments, including investigations into other use-cases and the analysis and development of analogous polynomial families for more general domains. As we show in Section 5, our method also supplies a new approach for related tasks, including the evaluation of the Fréchet derivative of matrix functions and the solving of other matrix equations. There is also a natural connection to the general evaluation of functions of matrices, which is thoroughly discussed in [5].

Figure 1 compares the errors in approximating the sign function via Akhiezer polynomials with the approximation error achieved via optimal rational approximation [1, Chapter 9] (see also [43, 58]) on various subsets of  $[-1, 1]$ . While we cannot expect to achieve the optimal rational convergence rate, the convergence rate is fast enough to yield a competitive algorithm in regimes where inversion is costly. Furthermore, this convergence rate can be determined a priori using only the intervals constituting the cut domain. It is governed by the level curves of the function  $e^{\operatorname{Re} \mathbf{g}(z)}$ , where  $\mathbf{g}(z)$  is defined above Lemma 3.2. The convergence rate of an approximation to a function  $f$  is governed by the largest value of  $c$  such that  $f$  can be analytically extended to the level set  $\operatorname{Re} \mathbf{g}(z) < c$ .

For the sign function, this maximal level set will correspond to a value  $c^*$  such that the level curves  $\operatorname{Re} \mathbf{g}(z) = c^*$  around each interval intersect. Thus, as  $c$  crosses  $c^*$ , we see a bifurcation of a connected level curve to a disconnected level curve, or vice versa. In Figure 2 we demonstrate this. We describe an inexpensive method to compute this intersection point, and thus the rate of convergence, in Section 3.3. These level curves are higher-genus analogs to Bernstein ellipses, as they govern the convergence rate of Akhiezer polynomial series on cut domains in the same manner that Bernstein ellipses govern the convergence rate of Chebyshev polynomial series on a single interval.

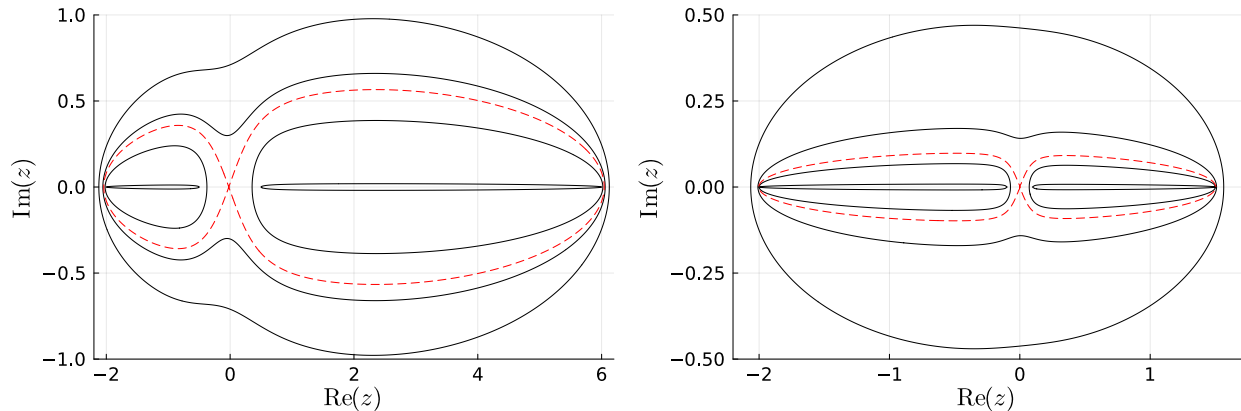


FIGURE 2. Generalized Bernstein ellipses for the cut domains  $[-2, -0.1] \cup [0.1, 1.5]$  (left) and  $[-2, -0.5] \cup [0.5, 6]$  (right). These are level curves of  $e^{\operatorname{Re}(z)}$  from Lemma 3.2. The red dashed line is the level curve where the curves around each interval first intersect,  $\operatorname{Re} \mathbf{g}(z) = c^*$ , and this governs the convergence rate of the Akhiezer polynomial approximation to the sign function on these domains.

**1.2. Related work.** Owing to the fact that  $\operatorname{sign}(\mathbf{H}) = \mathbf{H}(\mathbf{H}^2)^{-1/2}$ , iterative methods for computing matrix square roots can be used to evaluate the matrix sign function. While most of these algorithms employ inversion, the Newton–Schulz iteration is an exception. The iteration to compute the sign function is simple:

$$\mathbf{H}_{k+1} = \frac{1}{2} \mathbf{H}_k (3\mathbf{I} - \mathbf{H}_k^2).$$

This iteration achieves quadratic convergence, but it requires that  $\|\mathbf{I} - \mathbf{H}^2\| < 1$  in a subordinate matrix norm [31, Section 5.3]. By contrast, our method can be applied whenever the eigenvalues of  $\mathbf{H}$  are close to known intervals on the real axis. We discuss other connections with algorithms for the matrix square root in Section 5.3 and refer to [31] for a thorough survey.

Another inverse-free method for solving Sylvester matrix equations is given in [46]. Here, the authors develop a sketching method that greatly reduces the cost of employing a polynomial-based Krylov subspace method. While the convergence of the method is typically slow compared to rational Krylov methods, the savings induced by solving the much smaller sketched problems can make up for this since rational Krylov subspace methods are costly per iteration. We suspect that the use of the Akhiezer polynomials in concert with a sketched Krylov subspace method might lead to improved convergence rates for such schemes, but leave this for future work.

**1.3. Organization.** The rest of this paper is organized as follows. In Section 2, we establish notation for orthogonal polynomials and matrix functions and describe the Akhiezer iteration of [5]. In Section 3, we extend the Akhiezer iteration to an inverse-free iterative method for solving Sylvester matrix equations and analyze its complexity and convergence properties. In Section 4, we apply our method to solve integral equations and two-dimensional PDEs. In Section 5, we discuss other related applications. Code used to generate the plots in this paper can be found at [7].

## 2. ORTHOGONAL POLYNOMIALS AND THE AKHIEZER ITERATION

**2.1. Orthogonal polynomials and Cauchy integrals.** For our purposes, a weight function  $w$  is a nonnegative function supported on a finite union of disjoint intervals  $\Sigma$ ,  $\Sigma \subset \mathbb{R}$ , that is continuous and positive on the interior of  $\Sigma$  such that  $\int_{\Sigma} w(x) dx = 1$ . Consider a sequence of univariate monic polynomials  $(\pi_j(x))_{j=0}^{\infty}$  such that  $\pi_j$  has degree  $j$  for all  $j \in \mathbb{N}$ . These polynomials are said to be orthogonal with respect to a weight function  $w$  if

$$\langle \pi_j, \pi_k \rangle_{L_w^2(\Sigma)} = h_j \delta_{jk},$$

where  $h_j > 0$ ,  $\delta_{jk}$  is the Kronecker delta, and

$$(4) \quad \langle g, h \rangle_{L_w^2(\Sigma)} = \int_{\Sigma} g(x) \overline{h(x)} w(x) dx, \quad \|g\|_{L_w^2(\Sigma)} = \sqrt{\langle g, g \rangle_{L_w^2(\Sigma)}}.$$

The orthonormal polynomials  $(p_j(x))_{j=0}^{\infty}$  are defined by

$$p_j(x) = \frac{1}{\sqrt{h_j}} \pi_j(x),$$

for all  $j \in \mathbb{N}$ . The orthonormal polynomials satisfy the symmetric three-term recurrence

$$(5) \quad \begin{aligned} xp_0(x) &= a_0 p_0(x) + b_0 p_1(x), \\ xp_k(x) &= b_{k-1} p_{k-1}(x) + a_k p_k(x) + b_k p_{k+1}(x), \quad k \geq 1, \end{aligned}$$

where  $b_k > 0$  for all  $k$ . A general reference is [56].

Given a contour  $\Gamma \subset \mathbb{C}$  and a function  $f : \Gamma \rightarrow \mathbb{C}$ , the Cauchy transform  $\mathcal{C}_{\Gamma}$  is an operator that maps  $f$  to its Cauchy integral, i.e.,

$$\mathcal{C}_{\Gamma} f(z) = \frac{1}{2\pi i} \int_{\Gamma} \frac{f(s)}{s-z} ds, \quad z \in \mathbb{C} \setminus \Gamma.$$

The weighted Cauchy transforms  $\mathcal{C}_{\Sigma}[p_k w](z)$  will be important in the developments below.

**2.2. Functions of matrices.** The function of a matrix  $f(\mathbf{M})$  can be defined in several equivalent ways. For our purposes, the following two definitions will suffice:

**Definition 2.1.** *Suppose that  $f$  is a scalar-valued function defined on the spectrum of a diagonalizable matrix  $\mathbf{M} \in \mathbb{C}^{n \times n}$ , where  $\mathbf{M}$  is diagonalized as  $\mathbf{M} = \mathbf{V} \mathbf{\Lambda} \mathbf{V}^{-1}$ ,  $\mathbf{\Lambda} = \text{diag}(\lambda_1, \dots, \lambda_n)$ . Then,*

$$f(\mathbf{M}) := \mathbf{V} \text{diag}(f(\lambda_1), \dots, f(\lambda_n)) \mathbf{V}^{-1}.$$

With suitable assumptions on  $f$ , this definition can be extended to nondiagonalizable matrices via the Jordan normal form, but we will restrict most of our analysis to diagonalizable matrices. When  $f$  is appropriately analytic, we have the following equivalent definition [31, Theorem 1.12]:

**Definition 2.2.** *Suppose that  $\Gamma$  is a counterclockwise oriented curve that encloses the spectrum of  $\mathbf{M} \in \mathbb{C}^{n \times n}$  and that  $f$  is analytic in a region containing  $\Gamma$  and its interior. Then,*

$$f(\mathbf{M}) := \frac{1}{2\pi i} \int_{\Gamma} f(z) (z\mathbf{I} - \mathbf{M})^{-1} dz.$$

**2.3. The Akhiezer iteration.** Introduced in [5], the Akhiezer iteration<sup>1</sup> uses orthogonal polynomial series expansions to compute matrix functions. Given a finite union of disjoint intervals  $\Sigma \subset \mathbb{R}$  and a function  $f$  that is analytic in a region containing  $\Sigma$ , let  $p_0, p_1, \dots$  denote the orthonormal polynomials with respect to  $w$ . Then, for  $x \in \Sigma$ , a  $p_j$ -series expansion for  $f$  is given by

$$f(x) = \sum_{j=0}^{\infty} \alpha_j p_j(x), \quad \alpha_j = \langle f, p_j \rangle_{L_w^2(\Sigma)}.$$

For a matrix  $\mathbf{M}$  with eigenvalues on or near  $\Sigma$ , this extends to an iterative method for computing  $f(\mathbf{M})$  by truncating the series:

$$(6) \quad f(\mathbf{M}) = \sum_{j=0}^{\infty} \alpha_j p_j(\mathbf{M}) \approx \sum_{j=0}^k \alpha_j p_j(\mathbf{M}) =: \mathbf{F}_{k+1}.$$

<sup>1</sup>The method takes the name of Naum Akhiezer because, as discussed in Section 2.4, the classes of orthogonal polynomials that make the computation of the input data to the algorithm particularly efficient are often called *Akhiezer polynomials* [1, 22].

Of course, this requires methods to compute the coefficients  $\{\alpha_j\}_{j=0}^\infty$ . The matrix polynomials  $(p_j(\mathbf{A}))_{j=0}^\infty$  can be generated by (5),

$$(7) \quad \begin{aligned} p_0(\mathbf{M}) &= \mathbf{I}, \\ p_1(\mathbf{M}) &= \frac{1}{b_0}(\mathbf{M}p_0(\mathbf{M}) - a_0p_0(\mathbf{M})), \\ p_k(\mathbf{M}) &= \frac{1}{b_{k-1}}(\mathbf{M}p_{k-1}(\mathbf{M}) - a_{k-1}p_{k-1}(\mathbf{M}) - b_{k-2}p_{k-2}(\mathbf{M})), \quad k \geq 2. \end{aligned}$$

The coefficients  $\alpha_j$  cannot be computed analytically, in general, so let  $\Gamma, f$  be as in Definition 2.2. Then,

$$\alpha_j = \langle f, p_j \rangle_{L_w^2(\Sigma)} = \int_{\Sigma} f(x)p_j(x)w(x)dx = \int_{\Sigma} \left( \frac{1}{2\pi i} \int_{\Gamma} \frac{f(z)}{z-x} dz \right) p_j(x)w(x)dx.$$

After parameterizing  $\Gamma$  and applying a quadrature rule, such as a trapezoid rule [57], resulting in nodes  $\{z_j\}_{j=1}^m$  and weights  $\{w_j\}_{j=1}^m$ ,

$$\alpha_j \approx \int_{\Sigma} \frac{1}{2\pi i} \sum_{k=1}^m \frac{f(z_k)w_k}{z_k-x} p_j(x)w(x)dx = - \sum_{k=1}^m f(z_k)w_k \mathcal{C}_{\Sigma}[p_j w](z_k).$$

We see that in order to approximate the coefficients accurately, it suffices to be able to evaluate the weighted Cauchy integrals pointwise. Therefore, to apply the approximation (6), the recurrence coefficients and the pointwise evaluation of the Cauchy integrals of the desired orthonormal polynomials are all that is required. We refer to these input coefficients as the *Akhiezer data*.

With the Akhiezer data in hand, a precomputation, the approximation (6) can be implemented as the Akhiezer iteration as in Algorithm 1. See [5, Section 4] for the convergence analysis of the Akhiezer iteration, in particular when not all eigenvalues of  $\mathbf{M}$  lie in  $\Sigma$ .

---

**Algorithm 1:** Akhiezer iteration for matrix function approximation

---

**Input:**  $f, \mathbf{M}$ , and the Akhiezer data (functions to compute recurrence coefficients  $a_k, b_k$  and  $p_k$ -series coefficients  $\alpha_k$ ).

Set  $\mathbf{F}_0 = \mathbf{0}$ .

**for**  $k=0,1,\dots$  **do**

**if**  $k=0$  **then**

        Set  $\mathbf{P}_0 = \mathbf{I}$ .

**else if**  $k=1$  **then**

        Set  $\mathbf{P}_1 = \frac{1}{b_0}(\mathbf{M}\mathbf{P}_0 - a_0\mathbf{P}_0)$ .

**else**

        Set  $\mathbf{P}_k = \frac{1}{b_{k-1}}(\mathbf{M}\mathbf{P}_{k-1} - a_{k-1}\mathbf{P}_{k-1} - b_{k-2}\mathbf{P}_{k-2})$ .

**end**

    Set  $\mathbf{F}_{k+1} = \mathbf{F}_k + \alpha_k \mathbf{P}_k$ .

**if** converged **then**

**return**  $\mathbf{F}_{k+1}$ .

**end**

**end**

---

**Remark 2.3.** For most functions  $f$ , we choose  $\Gamma$  to be a collection of circles around each component of  $\Sigma$ , applying the trapezoid rule. Other contours, such as ellipses or hyperbolae, could provide better approximations in certain situations. We present an alternative approach specific to the sign function in Section 4.2.

**2.4. Computing the Akhiezer data.** If  $\Sigma$  is only a single interval, scaled and shifted Chebyshev polynomials and their simple recurrence are applicable. Formulae for the Cauchy integrals of Chebyshev polynomials can be found in [6, Section 4.1]. The method that results is closely related to the well-known Chebyshev iteration [38] in the case of  $f(z) = z^{-1}$ .

In [5] and [6], the authors present several methods for generating recurrence coefficients and the evaluation of Cauchy integrals. In particular, when  $\Sigma = [\beta_1, \gamma_1] \cup [\beta_2, \gamma_2]$ ,  $\gamma_1 < \beta_2$ , explicit formulae for the recurrence coefficients and Cauchy integrals of the so-called *Akhiezer polynomials* are found in terms of Jacobi elliptic and Jacobi theta functions [5, Section 3.1]. The two-interval Akhiezer polynomials are orthonormal polynomials with respect to the weight function [1, Chapter 10]

$$(8) \quad w(x) = \frac{1}{\pi} \mathbb{1}_{\Sigma}(x) \frac{\sqrt{x - \gamma_1}}{\sqrt{\gamma_2 - x} \sqrt{x - \beta_1} \sqrt{x - \beta_2}}.$$

**Remark 2.4.** *In the symmetric case  $\Sigma = [-1, -\beta] \cup [\beta, 1]$  ( $\beta > 0$ ), the Akhiezer polynomial recurrence coefficients can be shown to take a particularly simple form:*

$$a_n = (-1)^n \beta, \quad n \geq 0,$$

$$b_0 = \sqrt{\frac{1 - \beta^2}{2}}, \quad b_n = \frac{\sqrt{1 - \beta^2}}{2}, \quad n \geq 1.$$

*This can be accomplished, for example, by using continued fractions to show that (8) is the density of the spectral measure for the Jacobi matrix of recurrence coefficients.*

*If  $\gamma_1 + \beta_2 = \beta_1 + \gamma_2$ , the Akhiezer polynomial recurrence coefficients for  $\Sigma = [\beta_1, \gamma_1] \cup [\beta_2, \gamma_2]$ ,  $\gamma_1 < \beta_2$ , can be obtained by shifting and scaling these formulae.*

If  $\Sigma = \bigcup_{j=1}^{g+1} [\beta_j, \gamma_j]$  consists of more than two intervals, we refer the reader to the Riemann–Hilbert-based numerical method introduced in [6] and simplified in [5, Appendix A]. This method requires  $O(1)$  time to compute any given recurrence coefficient and  $O(1)$  time to evaluate any weighted Cauchy integral at a point. The method is particularly efficient for weight functions of the form

$$w(x) \propto \mathbb{1}_{\Sigma}(x) \frac{\sqrt{\gamma_{g+1} - x} \prod_{j=1}^{g+1} \sqrt{x - \beta_j}}{\prod_{j=1}^g \sqrt{x - \gamma_j}}.$$

Akhiezer’s formulae and the Riemann–Hilbert-based numerical method are implemented in the Julia package `RecurrenceCoefficients.jl` [4].

While these are our methods of choice, alternative methods do exist. An optimized  $O(N^2)$  algorithm for computing  $N$  pairs of recurrence coefficients for general orthogonal polynomials is given as RKPW in [29] and `lanczos.m` in [27]. More precisely, one uses a discretization of the inner product (4) as input to RKPW. In a different approach, [61], Wheeler constructs a weight function on two intervals such that the recurrence coefficients of the resulting orthogonal polynomials are 2-periodic and easily computable. Additionally, the annular polynomials of [47] in 1D yield orthogonal polynomials on symmetric intervals. In all of these cases, one may still need to compute Cauchy integrals of the orthonormal polynomials if the coefficients  $\alpha_j$  cannot be computed through other means. See [44, Chapter 7] for a discussion of this computation.

For  $\Sigma = \bigcup_{j=1}^{g+1} [\beta_j, \gamma_j]$ , a more general class of weight functions to which the forthcoming analysis applies is those of the form

$$(9) \quad w(x) = \sum_{j=1}^{g+1} \mathbb{1}_{[\beta_j, \gamma_j]}(x) h_j(x) \left( \sqrt{x - \beta_j} \right)^{c_j} \left( \sqrt{\gamma_j - x} \right)^{d_j}, \quad c_j, d_j \in \{-1, 1\},$$

where each  $h_j$  is positive on  $[\beta_j, \gamma_j]$  and has an analytic extension to a neighborhood of  $[\beta_j, \gamma_j]$ . The numerical method of [6] applies to all weight functions of this class.

## 3. AN INVERSE-FREE ITERATION FOR SYLVESTER EQUATIONS

We now turn to solving the Sylvester matrix equation (1). We assume that the spectrum of  $\mathbf{A}$  is contained in  $U_{\mathbf{A}}$  and that the spectrum of  $\mathbf{B}$  is contained in  $U_{\mathbf{B}}$ . Suppose  $\Xi = \alpha + e^{i\theta}\mathbb{R}$  is chosen such that the halfplanes  $H_{\mathbf{A}}$  and  $H_{\mathbf{B}}$  separated by  $\Xi$  contain  $U_{\mathbf{A}}$  and  $U_{\mathbf{B}}$ , respectively. Then, define

$$\text{sign} : \mathbb{C} \setminus \Xi \rightarrow \mathbb{C}, \quad \text{sign}(z) = \begin{cases} 1, & z \in H_{\mathbf{A}}, \\ -1, & z \in H_{\mathbf{B}}. \end{cases}$$

The choice of  $\Xi$  will affect the convergence rate estimates that appear later in this section.

The solution of (1) can be obtained as a subblock of the matrix sign function of the block matrix  $\mathbf{H}$  in (2). This follows from the factorizations

$$\begin{pmatrix} \mathbf{A} & \mathbf{0} \\ \mathbf{C} + \mathbf{B}\mathbf{X} & \mathbf{B} \end{pmatrix} = \begin{pmatrix} \mathbf{A} & \mathbf{0} \\ \mathbf{C} & \mathbf{B} \end{pmatrix} \begin{pmatrix} \mathbf{I}_n & \mathbf{0} \\ \mathbf{X} & \mathbf{I}_m \end{pmatrix}, \quad \begin{pmatrix} \mathbf{A} & \mathbf{0} \\ \mathbf{X}\mathbf{A} & \mathbf{B} \end{pmatrix} = \begin{pmatrix} \mathbf{I}_n & \mathbf{0} \\ \mathbf{X} & \mathbf{I}_m \end{pmatrix} \begin{pmatrix} \mathbf{A} & \mathbf{0} \\ \mathbf{0} & \mathbf{B} \end{pmatrix},$$

so (1) is equivalent to the equation

$$(10) \quad \mathbf{H} := \begin{pmatrix} \mathbf{A} & \mathbf{0} \\ \mathbf{C} & \mathbf{B} \end{pmatrix} = \begin{pmatrix} \mathbf{I}_n & \mathbf{0} \\ \mathbf{X} & \mathbf{I}_m \end{pmatrix} \begin{pmatrix} \mathbf{A} & \mathbf{0} \\ \mathbf{0} & \mathbf{B} \end{pmatrix} \begin{pmatrix} \mathbf{I}_n & \mathbf{0} \\ -\mathbf{X} & \mathbf{I}_m \end{pmatrix}.$$

When  $\sigma(\mathbf{A}) \subset [\beta_2, \gamma_2] \subset \mathbb{R}$ ,  $\sigma(\mathbf{B}) \subset [\beta_1, \gamma_1] \subset \mathbb{R}$ , and  $\gamma_1 < \beta_2$ , the Akhiezer iteration for  $\Sigma = [\beta_1, \gamma_1] \cup [\beta_2, \gamma_2]$ , as presented in Algorithm 1, can be directly applied to compute  $\text{sign}(\mathbf{H})$ , and thus solve the Sylvester equation (1). Note that despite its discontinuous nature, the sign function can always be defined so that it is analytic in a (disconnected) region containing  $\Sigma$ . We discuss this application and efficiency improvements in the following subsections.

**3.1. Isolating the lower left block.** Since only the lower left block of  $\text{sign}(\mathbf{H})$  is required to solve the Sylvester equation (1), we can reduce the necessary arithmetic operations using the following lemma.

**Lemma 3.1.** *Given a sequence of orthonormal polynomials  $(p_j(z))_{j=0}^{\infty}$  with three-term recurrence (5), the lower left block of  $p_j(\mathbf{H})$  where*

$$\mathbf{H} = \begin{pmatrix} \mathbf{A} & \mathbf{0} \\ \mathbf{C} & \mathbf{B} \end{pmatrix},$$

is given by

$$\mathbf{C}p_j(\mathbf{A}) + \mathbf{G}_j,$$

where  $\mathbf{G}_j$  satisfies

$$(11) \quad \begin{aligned} \mathbf{G}_0 &= -\mathbf{C}, \\ \mathbf{G}_1 &= \frac{1}{b_0}(\mathbf{G}_0\mathbf{A} + (a_0 + 1)\mathbf{C}), \\ \mathbf{G}_j &= \frac{1}{b_{j-1}}(\mathbf{G}_{j-1}\mathbf{A} + p_{j-1}(\mathbf{B})\mathbf{C} - a_{j-1}\mathbf{G}_{j-1} - b_{j-2}\mathbf{G}_{j-2}), \quad j \geq 2. \end{aligned}$$

*Proof.* For  $j = 0$ , the lower left block of  $p_0(\mathbf{H}) = \mathbf{I}$  is zero. Since  $p_0(\mathbf{A}) = \mathbf{I}$ ,  $\mathbf{C}p_0(\mathbf{A}) + \mathbf{G}_0 = \mathbf{0}$  when  $\mathbf{G}_0 = -\mathbf{C}$ . When  $j = 1$ , by (7), the lower left block of  $p_1(\mathbf{H})$  is given by  $\frac{1}{b_0}\mathbf{C}$ . Applying (7) to  $p_1(\mathbf{A})$ ,

$$\begin{aligned} \frac{1}{b_0}\mathbf{C} &= \frac{1}{b_0}\mathbf{C}(-a_0\mathbf{I} + (a_0 + 1)\mathbf{I}) = \frac{1}{b_0}\mathbf{C}(b_0p_1(\mathbf{A}) - \mathbf{A} + (a_0 + 1)\mathbf{I}) \\ &= \mathbf{C}p_1(\mathbf{A}) + \frac{1}{b_0}(\mathbf{G}_0\mathbf{A} + (a_0 + 1)\mathbf{C}). \end{aligned}$$

Using induction, let  $j \geq 2$  and assume that the lemma holds for  $p_{j-1}(\mathbf{H})$  and  $p_{j-2}(\mathbf{H})$ . Then,

$$p_{j-1}(\mathbf{H}) = \begin{pmatrix} p_{j-1}(\mathbf{A}) & \mathbf{0} \\ \mathbf{C}p_{j-1}(\mathbf{A}) + \mathbf{G}_{j-1} & p_{j-1}(\mathbf{B}) \end{pmatrix}, \quad p_{j-2}(\mathbf{H}) = \begin{pmatrix} p_{j-2}(\mathbf{A}) & \mathbf{0} \\ \mathbf{C}p_{j-2}(\mathbf{A}) + \mathbf{G}_{j-2} & p_{j-2}(\mathbf{B}) \end{pmatrix}.$$



Applying (7) and noting that matrices commute with polynomials of themselves, the lower left block of  $p_j(\mathbf{H})$  is given by

$$\begin{aligned} & \frac{1}{b_{j-1}} (\mathbf{C}p_{j-1}(\mathbf{A})\mathbf{A} + \mathbf{G}_{j-1}\mathbf{A} + p_{j-1}(\mathbf{B})\mathbf{C} - a_{j-1}\mathbf{C}p_{j-1}(\mathbf{A}) - a_{j-1}\mathbf{G}_{j-1} - b_{j-2}\mathbf{C}p_{j-2}(\mathbf{A}) - b_{j-2}\mathbf{G}_{j-2}) \\ & = \mathbf{C}p_j(\mathbf{A}) + \frac{1}{b_{j-1}} (\mathbf{G}_{j-1}\mathbf{A} + p_{j-1}(\mathbf{B})\mathbf{C} - a_{j-1}\mathbf{G}_{j-1} - b_{j-2}\mathbf{G}_{j-2}), \end{aligned}$$

which completes the proof.  $\square$

Lemma 3.1 allows the Akhiezer iteration applied to Sylvester equations to be implemented such that full block  $(n + m) \times (n + m)$  matrix-matrix multiplications are no longer needed; however, the matrix polynomials  $p_j(\mathbf{A})$  and  $p_j(\mathbf{B})$  are both still required to compute the desired lower left block. Thus, recurrences for these matrix polynomials and the approximate solution can be run in parallel, effectively decoupling the large matrix-matrix product into five smaller ones. A Sylvester equation solver based on this decoupling can be implemented as in Algorithm 2.

---

**Algorithm 2:** Decoupled  $\mathbf{XA} - \mathbf{BX} = \mathbf{C}$  solver via the Akhiezer iteration

---

**Input:** Matrices  $\mathbf{A}, \mathbf{B}, \mathbf{C}$  and the Akhiezer data (functions to compute recurrence coefficients  $a_k, b_k$  and  $p_k$ -series coefficients  $\alpha_k$  for the sign function).

Set  $\mathbf{X}_0 = 0$ .

**for**  $k=0, 1, \dots$  **do**

**if**  $k=0$  **then**

    Set  $p_0(\mathbf{A}) = \mathbf{I}$ .

    Set  $p_0(\mathbf{B}) = \mathbf{I}$ .

    Set  $\mathbf{G}_0 = -\mathbf{C}$ .

**else if**  $k=1$  **then**

    Set  $p_1(\mathbf{A}) = \frac{1}{b_0}(p_0(\mathbf{A})\mathbf{A} - a_0p_0(\mathbf{A}))$ .

    Set  $p_1(\mathbf{B}) = \frac{1}{b_0}(\mathbf{B}p_0(\mathbf{B}) - a_0p_0(\mathbf{B}))$ .

    Set  $\mathbf{G}_1 = \frac{1}{b_0}(\mathbf{G}_0\mathbf{A} + (a_0 + 1)\mathbf{C})$ .

**else**

    Set  $p_k(\mathbf{A}) = \frac{1}{b_{k-1}}(p_{k-1}(\mathbf{A})\mathbf{A} - a_{k-1}p_{k-1}(\mathbf{A}) - b_{k-2}p_{k-2}(\mathbf{A}))$ .

    Set  $p_k(\mathbf{B}) = \frac{1}{b_{k-1}}(\mathbf{B}p_{k-1}(\mathbf{B}) - a_{k-1}p_{k-1}(\mathbf{B}) - b_{k-2}p_{k-2}(\mathbf{B}))$ .

    Set  $\mathbf{G}_k = \frac{1}{b_{k-1}}(\mathbf{G}_{k-1}\mathbf{A} + p_{k-1}(\mathbf{B})\mathbf{C} - a_{k-1}\mathbf{G}_{k-1} - b_{k-2}\mathbf{G}_{k-2})$ .

**end**

  Set  $\mathbf{X}_{k+1} = \mathbf{X}_k + \frac{\alpha_k}{2}(\mathbf{C}p_k(\mathbf{A}) + \mathbf{G}_k)$ .

**if** converged **then**

**return**  $\mathbf{X}_{k+1}$ .

**end**

**end**

---

**3.2. Compression and low-rank structure.** In the case where the data matrix  $\mathbf{C}$  in (1) is low rank, Algorithm 2 is suboptimal in that it requires full matrix-matrix products. Moreover, it is known that when the rank of  $\mathbf{C}$  is bounded above by a small number  $r$  and  $\mathbf{A}$  and  $\mathbf{B}$  are normal<sup>2</sup> with well-separated spectral sets, then  $\mathbf{X}$  is well-approximated by a low-rank matrix [12]. We say that such a matrix is *numerically* of low rank. Specifically, we say that  $\mathbf{X}$  is numerically of rank  $k$  with respect to the tolerance  $0 < \epsilon < 1$  if the  $(k + 1)$ st singular value of  $\mathbf{X}$  is bounded above by  $\|\mathbf{X}\|_F \epsilon$ , where  $\|\diamond\|_F$  denotes the standard Frobenius norm. Throughout this paper, we take

<sup>2</sup>Generalizations for the nonnormal case are also known [12].

$\epsilon = 10^{-13}$ . Rather than constructing  $\mathbf{X}_k$  outright, it is preferable to construct low-rank factors  $\mathbf{W}_k \mathbf{Z}_k = \mathbf{X}_k$ .

Here, we suppose we are given a low rank factorization of  $\mathbf{C}$  in (1), and so consider the equation (12)

$$\mathbf{X}\mathbf{A} - \mathbf{B}\mathbf{X} = \mathbf{U}\mathbf{V},$$

where  $\mathbf{U} \in \mathbb{C}^{m \times r}$  and  $\mathbf{V} \in \mathbb{C}^{r \times n}$  are given with  $r$  much smaller than  $m$  and  $n$ .

To incorporate the low-rank structure into our iteration, we note that the recurrence (7) can be left- and right-multiplied, respectively, giving

$$\begin{aligned} \mathbf{V}p_0(\mathbf{A}) &= \mathbf{V}, \\ \mathbf{V}p_1(\mathbf{A}) &= \frac{1}{b_0}(\mathbf{V}p_0(\mathbf{A})\mathbf{A} - a_0\mathbf{V}p_0(\mathbf{A})), \\ \mathbf{V}p_k(\mathbf{A}) &= \frac{1}{b_{k-1}}(\mathbf{V}p_{k-1}(\mathbf{A})\mathbf{A} - a_{k-1}\mathbf{V}p_{k-1}(\mathbf{A}) - b_{k-2}\mathbf{V}p_{k-2}(\mathbf{A})), \quad k \geq 2, \end{aligned}$$

and

$$\begin{aligned} p_0(\mathbf{B})\mathbf{U} &= \mathbf{U}, \\ p_1(\mathbf{B})\mathbf{U} &= \frac{1}{b_0}(\mathbf{B}p_0(\mathbf{B})\mathbf{U} - a_0p_0(\mathbf{B})\mathbf{U}), \\ p_k(\mathbf{B})\mathbf{U} &= \frac{1}{b_{k-1}}(\mathbf{B}p_{k-1}(\mathbf{B})\mathbf{U} - a_{k-1}p_{k-1}(\mathbf{B})\mathbf{U} - b_{k-2}p_{k-2}(\mathbf{B})\mathbf{U}), \quad k \geq 2. \end{aligned}$$

By computing with only these recurrence formulae, we circumvent the need to compute the full diagonal blocks of  $p_j(\mathbf{H})$ , greatly reducing the size of the needed matrix-matrix products when  $r$  is small. Letting  $\mathbf{G}_j = \mathbf{J}_j \mathbf{K}_j$ , we write the recurrence (11) in block low-rank form as

$$\begin{aligned} \mathbf{J}_0 \mathbf{K}_0 &= \mathbf{G}_0 = -\mathbf{U}\mathbf{V}, \\ \mathbf{J}_1 \mathbf{K}_1 &= \mathbf{G}_1 = \frac{1}{b_0} \begin{pmatrix} \mathbf{J}_0 & (a_0 + 1)\mathbf{U} \end{pmatrix} \begin{pmatrix} \mathbf{K}_0 \mathbf{A} \\ \mathbf{V} \end{pmatrix}, \\ \mathbf{J}_j \mathbf{K}_j &= \mathbf{G}_j = \frac{1}{b_{j-1}} \begin{pmatrix} \mathbf{J}_{j-1} & p_{j-1}(\mathbf{B})\mathbf{U} & -a_{j-1}\mathbf{J}_{j-1} & -b_{j-2}\mathbf{J}_{j-2} \end{pmatrix} \begin{pmatrix} \mathbf{K}_{j-1} \mathbf{A} \\ \mathbf{V} \\ \mathbf{K}_{j-1} \\ \mathbf{K}_{j-2} \end{pmatrix}, \quad j \geq 2. \end{aligned}$$

Then, letting  $\mathbf{X}_k = \mathbf{W}_k \mathbf{Z}_k$ , the update step from Algorithm 2 can be written as

$$\mathbf{W}_{k+1} \mathbf{Z}_{k+1} = \mathbf{X}_{k+1} = \begin{pmatrix} \mathbf{W}_k & \frac{\alpha_k}{2} \mathbf{U} & \frac{\alpha_k}{2} \mathbf{J}_k \end{pmatrix} \begin{pmatrix} \mathbf{Z}_k \\ \mathbf{V} p_k(\mathbf{A}) \\ \mathbf{K}_k \end{pmatrix}.$$

These relations allow Algorithm 2 to be decoupled such that two matrices,  $\mathbf{W}_k$  and  $\mathbf{Z}_k$ , are updated separately and the approximate solution is the product of the two. However, their direct use is hampered by the fact that the number of rows or columns grows rapidly with  $k$ . To address this, we compress these matrices to their numerical rank as needed. A simple compression method based on the QR/LQ and singular value decompositions (SVD) is given in Algorithm 3.

Given a method that compresses the matrices  $\mathbf{J}_k \mathbf{K}_k$  and  $\mathbf{W}_k \mathbf{Z}_k$  to match their numerical rank, the above recurrence relations allow Algorithm 2 to be rewritten so that only low-rank matrix-matrix products and compression steps are necessary to compute a solution. An implementation of this is given as Algorithm 4.

This algorithm chooses compression tolerances in a manner that depends on the iteration step which we now motivate. Since  $\mathbf{X}$  will be numerically of low rank, we expect the approximate solution  $\mathbf{W}_k \mathbf{Z}_k$  of Algorithm 4 to be numerically of low rank for all  $k$ . However, we have no reason to expect the lower left block of  $p_j(\mathbf{H})$  to be numerically of low rank for large  $j$ , meaning that as the iteration count increases, a low-rank object is being constructed out of increasingly higher-rank objects. In Figure 3, we plot the numerical ranks of both the component pieces  $\mathbf{J}_k \mathbf{K}_k$  and

**Algorithm 3:** Simple compression of  $(\mathbf{J}, \mathbf{K})$ COMPRESS( $\mathbf{J}, \mathbf{K}, \epsilon$ )**Input:** Matrices  $\mathbf{J} \in \mathbb{C}^{m \times n}$ ,  $\mathbf{K} \in \mathbb{C}^{n \times \ell}$  and tolerance  $\epsilon$ .Run QR on  $\mathbf{J}$  to get  $\mathbf{Q}_J \mathbf{R} = \mathbf{J}$ .Run LQ on  $\mathbf{K}$  to get  $\mathbf{LQ}_K = \mathbf{K}$ .Run SVD on  $\mathbf{RL}$  to get  $\mathbf{U}\Sigma\mathbf{V} = \mathbf{RL}$ .Truncate  $\Sigma$  so that all remaining singular values satisfy  $\sigma_j^2 / \sum_j \sigma_j^2 < \epsilon$ , leaving  $\tilde{\Sigma} \in \mathbb{R}^{k \times k}$ .Truncate rows or columns of  $\mathbf{U}$  and  $\mathbf{V}$  as appropriate, leaving  $\tilde{\mathbf{U}} \in \mathbb{C}^{m \times k}$  and  $\tilde{\mathbf{V}} \in \mathbb{C}^{k \times \ell}$ .Return  $\tilde{\mathbf{J}} = \mathbf{Q}_J \tilde{\mathbf{U}} \tilde{\Sigma}^{1/2}$ ,  $\tilde{\mathbf{K}} = \tilde{\Sigma}^{1/2} \tilde{\mathbf{V}} \mathbf{Q}_K$ .**Algorithm 4:** Low-rank  $\mathbf{XA} - \mathbf{BX} = \mathbf{UV}$  solver using the Akhiezer iteration**Input:** Matrices  $\mathbf{A}, \mathbf{B}, \mathbf{U}, \mathbf{V}$ , the Akhiezer data (functions to compute recurrence coefficients  $a_k, b_k$  and  $p_k$ -series coefficients  $\alpha_k$  for the sign function), computed decay rate  $\varrho$  and constant  $c$  as in Section 3.3, and compression tolerance  $\epsilon$ .Initialize  $\mathbf{W}_0$  and  $\mathbf{Z}_0$  to be empty.**for**  $k=0, 1, \dots$  **do**  **if**  $k=0$  **then**    Set  $\mathbf{V}p_0(\mathbf{A}) = \mathbf{V}$ .    Set  $p_0(\mathbf{B})\mathbf{U} = \mathbf{U}$ .    Set  $\mathbf{J}_0 = -\mathbf{U}$ .    Set  $\mathbf{K}_0 = \mathbf{V}$ .  **else if**  $k=1$  **then**    Set  $\mathbf{V}p_1(\mathbf{A}) = \frac{1}{b_0}(\mathbf{V}p_0(\mathbf{A})\mathbf{A} - a_0\mathbf{V}p_0(\mathbf{A}))$ .    Set  $p_1(\mathbf{B})\mathbf{U} = \frac{1}{b_0}(\mathbf{B}p_0(\mathbf{B})\mathbf{U} - a_0p_0(\mathbf{B})\mathbf{U})$ .    Set  $\mathbf{J}_1 = \frac{1}{b_0}(\mathbf{J}_0 - (a_0 + 1)\mathbf{U})$ .    Set  $\mathbf{K}_1 = \begin{pmatrix} \mathbf{K}_0 \mathbf{A} \\ \mathbf{V} \end{pmatrix}$ .  **else**    Set  $\mathbf{V}p_k(\mathbf{A}) = \frac{1}{b_{k-1}}(\mathbf{V}p_{k-1}(\mathbf{A})\mathbf{A} - a_{k-1}\mathbf{V}p_{k-1}(\mathbf{A}) - b_{k-2}\mathbf{V}p_{k-2}(\mathbf{A}))$ .    Set  $p_k(\mathbf{B})\mathbf{U} = \frac{1}{b_{k-1}}(\mathbf{B}p_{k-1}(\mathbf{B})\mathbf{U} - a_{k-1}p_{k-1}(\mathbf{B})\mathbf{U} - b_{k-2}p_{k-2}(\mathbf{B})\mathbf{U})$ .    Set  $\mathbf{J}_k = \frac{1}{b_{k-1}}(\mathbf{J}_{k-1} - p_{k-1}(\mathbf{B})\mathbf{U} - a_{k-1}\mathbf{J}_{k-1} - b_{k-2}\mathbf{J}_{k-2})$ .    Set  $\mathbf{K}_k = \begin{pmatrix} \mathbf{K}_{k-1} \mathbf{A} \\ \mathbf{V} \\ \mathbf{K}_{k-1} \\ \mathbf{K}_{k-2} \end{pmatrix}$ .  **end**Set  $\mathbf{J}_k, \mathbf{K}_k = \text{COMPRESS}(\mathbf{J}_k, \mathbf{K}_k, \frac{\varrho^k \epsilon}{c})$ .Set  $\mathbf{W}_{k+1} = \begin{pmatrix} \mathbf{W}_k & \frac{\alpha_k}{2} \mathbf{U} \\ & \frac{\alpha_k}{2} \mathbf{J}_k \end{pmatrix}$ .Set  $\mathbf{Z}_{k+1} = \begin{pmatrix} \mathbf{Z}_k \\ \mathbf{V}p_k(\mathbf{A}) \\ \mathbf{K}_k \end{pmatrix}$ .Set  $\mathbf{W}_{k+1}, \mathbf{Z}_{k+1} = \text{COMPRESS}(\mathbf{W}_{k+1}, \mathbf{Z}_{k+1}, \epsilon)$ .**if** converged **then**  **return**  $\mathbf{W}_{k+1}, \mathbf{Z}_{k+1}$ .**end****end**

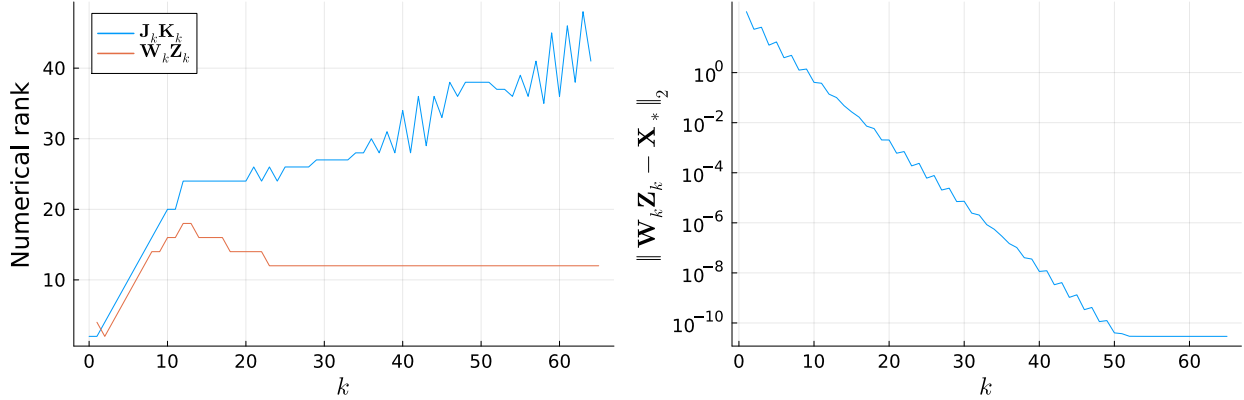


FIGURE 3. Numerical rank of the iterates of Algorithm 4 with unweighted compression (left) and error of the approximation at each iteration against the true solution  $\mathbf{X}_*$  of (12), computed via `sylvester`, the built-in Julia implementation of the Bartels–Stewart algorithm [9]. Here,  $\mathbf{A} \in \mathbb{R}^{1000 \times 1000}$ ,  $\mathbf{B} \in \mathbb{R}^{900 \times 900}$ ,  $\mathbf{UV}$  is rank 2, and the numerical solution appears to have numerical rank 12.

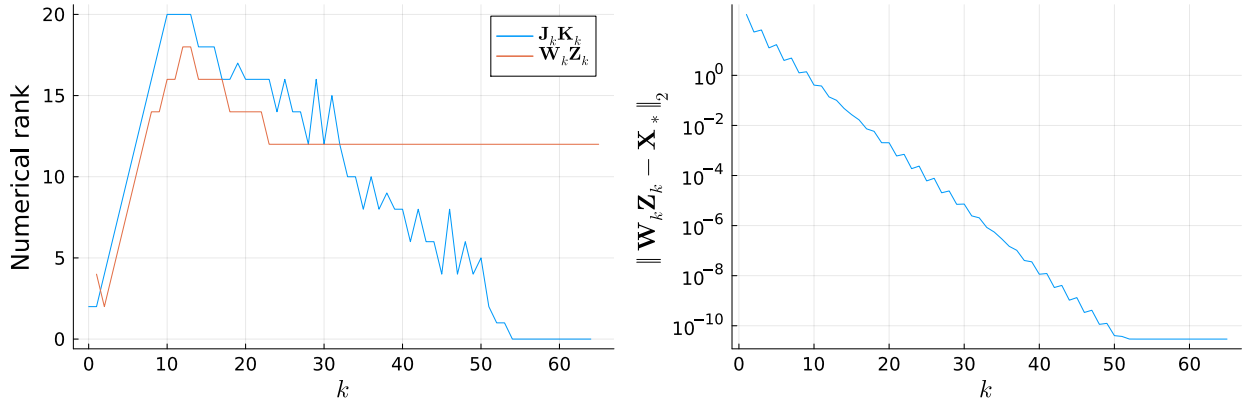


FIGURE 4. Numerical rank of the iterates of Algorithm 4 with weighted compression (left) and error of the approximation at each iteration against the true solution  $\mathbf{X}_*$  (right). The problem is the same as that of Figure 3, and only the tolerance for the compression of  $\mathbf{J}_k \mathbf{K}_k$  was changed.

of the approximate solution  $\mathbf{W}_k \mathbf{Z}_k$  for an example problem where  $\mathbf{A} \in \mathbb{R}^{1000 \times 1000}$ ,  $\sigma(\mathbf{A}) \subset [2, 3]$ ,  $\mathbf{B} \in \mathbb{R}^{900 \times 900}$ ,  $\sigma(\mathbf{B}) \subset [-1.8, -0.5]$ ,  $\mathbf{U} \in \mathbb{R}^{900 \times 2}$ , and  $\mathbf{V} \in \mathbb{R}^{2 \times 1000}$ . The numerical rank of  $\mathbf{J}_k \mathbf{K}_k$  appears to grow while the numerical rank of  $\mathbf{W}_k \mathbf{Z}_k$  converges to that of the true solution. The reason for this is that  $\mathbf{J}_k \mathbf{K}_k$  is always scaled by a  $p_j$ -series coefficient  $\alpha_k$  when  $\mathbf{W}_k \mathbf{Z}_k$  is updated, but these coefficients decay exponentially as  $k$  increases [5, Lemma 4.10]. Due to this decay and the fact that  $\mathbf{J}_k \mathbf{K}_k$  is used to generate  $\mathbf{J}_{k+1} \mathbf{K}_{k+1}$ , one may consider enlarging the tolerance (as in Algorithm 3) in the compression of  $\mathbf{J}_k \mathbf{K}_k$  by the decay rate of  $|\alpha_k|$ . See Section 3.3 for a full discussion of this. In Figure 4, we plot the numerical rank of  $\mathbf{J}_k \mathbf{K}_k$  and  $\mathbf{W}_k \mathbf{Z}_k$  when the compression of  $\mathbf{J}_k \mathbf{K}_k$  is weighted by the decay rate. We observe that the rank of  $\mathbf{J}_k \mathbf{K}_k$  now decays as the rank of  $\mathbf{W}_k \mathbf{Z}_k$  converges to that of the true solution, but the convergence rate of the iteration is not noticeably affected.

**3.3. Parameter tuning and heuristics.** We use  $\mathfrak{g}$  to denote the Green’s function with pole at infinity, exterior to  $\Sigma$ ; see [5, Appendix A], for example, for its explicit construction. This function satisfies  $\operatorname{Re} \mathfrak{g}(z) = 0$  for  $z \in \Sigma$ , and  $e^{\mathfrak{g}(z)}$  is a conformal map from  $\mathbb{C} \setminus \Sigma$  to the exterior of the unit

disk. A method to compute  $\mathbf{g}$  for a collection of disjoint intervals  $\Sigma$  is described in [6, Section 4.2]. For the relevant two interval case, [5, Section 4.1.1] gives an explicit formula that may be evaluated directly. Both methods are implemented in [4]. We plot the level curves of this function in Figure 2. As discussed in Section 1, these level curves are a higher genus analog of Bernstein ellipses. Define

$$(13) \quad B_\varrho = \{z \in \mathbb{C} : e^{\operatorname{Re} \mathbf{g}(z)} < \varrho\}, \quad \varrho > 1.$$

For all  $\varrho > 1$ ,  $B_\varrho$  is an open set that contains  $\Sigma$ . We have the following lemma from [5] that will inform compression thresholds in our algorithm:

**Lemma 3.2.** *Let  $\Sigma = \bigcup_{j=1}^{g+1} [\beta_j, \gamma_j] \subset \mathbb{R}$  be a union of disjoint intervals and assume that  $f(z)$  is analytic for  $z \in B_\varrho$ ,  $\varrho > 1$ , and  $|f(z)| \leq M$  for  $z \in B_\varrho$ . Let  $w$  be a weight function of the form (9) and denote the corresponding orthonormal polynomials by  $(p_j(x))_{j=0}^\infty$ . Then, there exists a constant  $C > 0$ , independent of  $f$ , such that*

$$|\langle f, p_\ell \rangle_{L_w^2(\Sigma)}| \leq CM\varrho^{-\ell}, \quad \ell \in \mathbb{N}.$$

To determine the convergence rate  $\varrho^{-1}$  when  $f$  is the sign function, consider  $\Sigma = [\beta_1, \gamma_1] \cup [\beta_2, \gamma_2]$ ,  $\gamma_1 < \beta_2$ . The largest value of  $\varrho$  such that  $f(z) = \operatorname{sign}(z)$  can be defined so that it is analytic in  $B_\varrho$  will correspond to the value of  $\varrho$  where the disjoint level curves around  $[\beta_1, \gamma_1]$  and  $[\beta_2, \gamma_2]$  first intersect, as  $\varrho$  increases. This intersection point is precisely the unique local maximum of  $\operatorname{Re} \mathbf{g}(z)$  for  $z \in [\gamma_1, \beta_2]$ . The location of this intersection follows from [5, Appendix A] and is given by<sup>3</sup>

$$z^* = \frac{\int_{\gamma_1}^{\beta_2} \frac{z dz}{\sqrt{z-\beta_1}\sqrt{z-\gamma_1}\sqrt{z-\beta_2}\sqrt{z-\gamma_2}}}{\int_{\gamma_1}^{\beta_2} \frac{dz}{\sqrt{z-\beta_1}\sqrt{z-\gamma_1}\sqrt{z-\beta_2}\sqrt{z-\gamma_2}}}.$$

Given the intersection point  $z^*$  of the level curves, we have the following bound on the coefficients of a  $p_j$ -series expansion of the sign function:

$$|\alpha_j| = |\langle \operatorname{sign}, p_j \rangle_{L_w^2(\Sigma)}| \leq C\varrho^{-j}, \quad \varrho = e^{\operatorname{Re} \mathbf{g}(z^*)},$$

for some constant  $C > 0$  that cannot in general be computed. We use this bound to inform a heuristic for the weighted compression described in Section 3.2. We find that the weighted compression step tends to behave well when the tolerance is simply multiplied by  $\frac{\varrho^k}{c}$  at iteration  $k$  where  $\varrho$  is computed a priori and  $c$  is a chosen constant taken in place of  $C$ . Since the coefficients  $\alpha_j$  are computed a priori, one may simply select  $c$  such that  $|\alpha_j| \leq c\varrho^{-j}$  by plotting or other means; however, we find that it typically suffices to take  $c = 5$ . One can always plot the series coefficients if uncertain. See Figure 5 for plots of the coefficients against the heuristic with  $c = 5$ .

**3.4. Convergence and stopping criteria.** In this subsection, we present a convergence analysis that is largely a simplified version of that of [5, Section 4] under the additional assumption that the eigenvalues of the matrix lie in the interior of  $\Sigma$ . Some results are reproduced directly without proof. We begin with the following definition to simplify the analysis:

**Definition 3.3.** *We say that a matrix is generic if it is diagonalizable and none of its eigenvalues lie at endpoints of  $\Sigma$ .*

See [5, Section 4.1.1] for remarks on how the analysis can be extended to nongeneric matrices. The following lemma describes the relevant behavior of the polynomials:

<sup>3</sup>We note that  $z^* = 0$  when the intervals are symmetric about  $z = 0$ . A formula for  $z^*$  may also be obtained by differentiating the formulae in [5, Section 3.1 and 4.1.1]; however, given the ease of computing  $\mathbf{g}$  via the formula in [5, Section 4.1.1], we find that it is fastest and easiest to find the intersection point  $z^*$  via a numerical method such as the golden-section search.

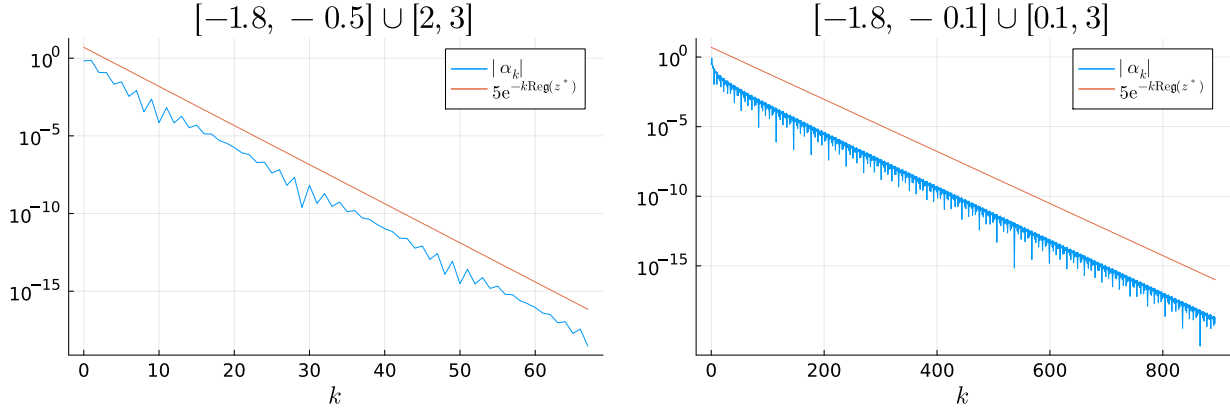


FIGURE 5. Modulus of the coefficients of an Akhiezer polynomial series approximation to the sign function on  $[-1.8, -0.5] \cup [2, 3]$  (left) and  $[-1.8, -0.1] \cup [0.1, 3]$  (right) plotted against the convergence rate heuristic with  $c = 5$  until the heuristic is smaller than  $10^{-16}$ .

**Lemma 3.4.** *Let  $\Sigma = \bigcup_{j=1}^{g+1} [\beta_j, \gamma_j] \subset \mathbb{R}$  be a union of disjoint intervals and let  $w$  be a weight function of the form (9). Denote the corresponding orthonormal polynomials by  $(p_j(z))_{j=0}^{\infty}$ , fix  $\epsilon > 0$ , and set  $V = \{z \in \mathbb{C} : |z - \beta_j| \geq \epsilon, |z - \gamma_j| \geq \epsilon, j = 1, \dots, g + 1\}$ . Then,*

$$p_n(z) = \hat{\delta}_n(z)e^{ng(z)}, \quad 2\pi i C_{\Sigma} [p_n w](z) = \delta_n(z)e^{-ng(z)}, \quad z \in V,$$

where  $\delta_n(z)$  and  $\hat{\delta}_n(z)$  are uniformly bounded in both  $n$  and  $z \in V$ .

In the following,  $\|\diamond\|_2$  will denote the Euclidean 2-norm and the induced matrix norm.

**Theorem 3.5.** *Under the assumptions of Lemma 3.2, suppose that  $\mathbf{M}$  is generic and  $\sigma(\mathbf{M}) \subset \Sigma$ . Then, there exists a constant  $C' > 0$ , independent of  $f$ , such that the approximation (6) satisfies*

$$\|f(\mathbf{M}) - \mathbf{F}_k\|_2 \leq C' M \|\mathbf{V}\|_2 \|\mathbf{V}^{-1}\|_2 \frac{\varrho^{-k}}{1 - \varrho^{-1}},$$

where  $\mathbf{M}$  is diagonalized as  $\mathbf{M} = \mathbf{V}\mathbf{\Lambda}\mathbf{V}^{-1}$ .

*Proof.* By the triangle inequality,

$$\begin{aligned} \|f(\mathbf{M}) - \mathbf{F}_k\|_2 &= \left\| \sum_{j=k}^{\infty} \alpha_j p_j(\mathbf{M}) \right\|_2 \leq \sum_{j=k}^{\infty} CM \varrho^{-j} \|\mathbf{V}\|_2 \|p_j(\mathbf{\Lambda})\|_2 \|\mathbf{V}^{-1}\|_2 \\ &= CM \|\mathbf{V}\|_2 \|\mathbf{V}^{-1}\|_2 \sum_{j=k}^{\infty} \varrho^{-j} \max_{\lambda \in \sigma(\mathbf{M})} |p_j(\lambda)|. \end{aligned}$$

Since  $\lambda$  lies in the interior of  $\Sigma$  for all  $\lambda \in \sigma(\mathbf{M})$ , by Lemma 3.4, there exists some constant  $c$  such that

$$|p_j(\lambda)| = \left| \hat{\delta}_j(\lambda) \right| e^{j \operatorname{Re} g(\lambda)} \leq c,$$

for all  $j$  and  $\lambda \in \sigma(\mathbf{M})$ . The theorem follows from using  $C' = cC$  and

$$\sum_{j=k}^{\infty} \varrho^{-j} = \frac{\varrho^{-k}}{1 - \varrho^{-1}}.$$

□

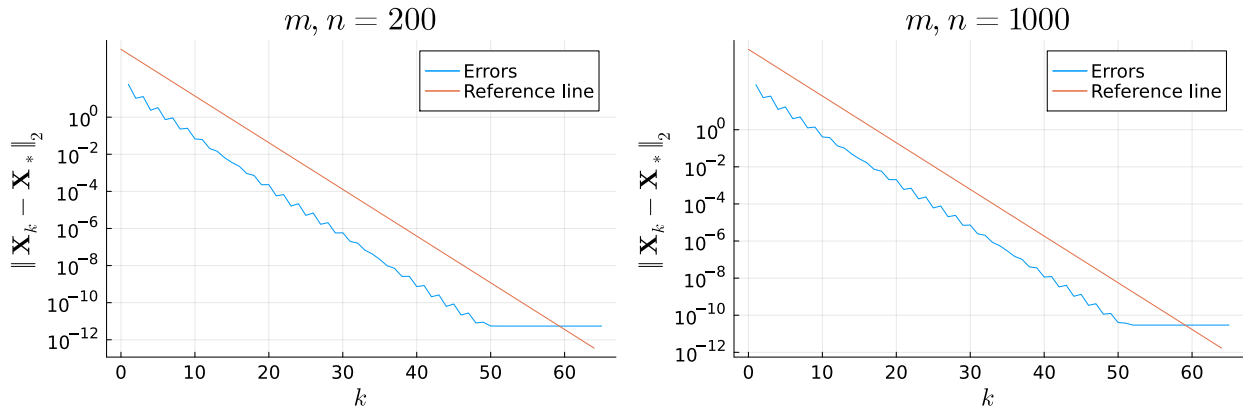


FIGURE 6. 2-norm error for  $\mathbf{X}_k$  against the true solution  $\mathbf{X}_*$  to (1) (computed via `sylvester` in Julia) at each iteration where  $\mathbf{C}$  is rank 2,  $\mathbf{A}, \mathbf{B} \in \mathbb{R}^{200 \times 200}$  (left),  $\mathbf{A}, \mathbf{B} \in \mathbb{R}^{1000 \times 1000}$  (right),  $\sigma(\mathbf{A}) \subset [2, 3]$ , and  $\sigma(\mathbf{B}) \subset [-1.8, -0.5]$ . Here, the reference line denotes the convergence rate heuristic (16) with  $D_{\mathbf{H}}$  replaced by the hypothesized upper bound  $10(n + m)$ .

Theorem 3.5 implies that the Akhiezer iteration converges, at worst, at a geometric rate given by  $\varrho^{-1}$ . If  $f$  is the sign function, then  $M = 1$ . This theorem then implies that there exists some constant  $D_{\mathbf{M}} > 0$ , dependent on the eigenvectors of  $\mathbf{M}$ , such that

$$(14) \quad \|\text{sign}(\mathbf{M}) - \mathbf{F}_k\|_2 \leq D_{\mathbf{M}} \frac{\varrho^{-k}}{1 - \varrho^{-1}}.$$

In particular, for a given tolerance  $\epsilon > 0$ , we require

$$(15) \quad k = \left\lceil -\log_{\varrho} \frac{\epsilon(1 - \varrho^{-1})}{D_{\mathbf{M}}} \right\rceil,$$

iterations to ensure that

$$\|\text{sign}(\mathbf{M}) - \mathbf{F}_k\|_2 < \epsilon.$$

Since it depends on eigenvectors and orthogonal polynomial asymptotics,  $D_{\mathbf{M}}$  cannot be cheaply computed in general. Like with the orthogonal polynomial series coefficients, we hypothesize an upper bound  $D_{\mathbf{M}} \leq 10\ell$  for generic  $\mathbf{M} \in \mathbb{C}^{\ell \times \ell}$ . One can always run more iterations if this hypothesized bound appears insufficient.

We note that in finite-precision, the iteration will saturate when the coefficients  $\alpha_j$  reach machine precision  $\epsilon_{\text{mach}}$ . We use

$$k = \left\lceil \min \left\{ -\log_{\varrho} \left( \frac{\epsilon(1 - \varrho^{-1})}{10\ell} \right), -\log_{\varrho} \left( \frac{\epsilon_{\text{mach}}}{5} \right) \right\} \right\rceil,$$

iterations in place of (15).

Now, consider  $\mathbf{H}$  from (10) and let  $\mathbf{X}^*$  denote the true solution of the Sylvester equation (1). Of course, the error of interest is  $\mathbf{X}_k - \mathbf{X}^*$ , not  $\text{sign}(\mathbf{H}) - \mathbf{F}_k$ . Naively, we have

$$(16) \quad \|\mathbf{X}_k - \mathbf{X}^*\|_2 \leq \frac{1}{2} \|\text{sign}(\mathbf{H}) - \mathbf{F}_k\|_2 \leq \frac{D_{\mathbf{H}}}{2} \frac{\varrho^{-k}}{1 - \varrho^{-1}}.$$

Empirically, we find that the error in this iteration does not decay faster than the geometric rate given by  $\varrho^{-1}$ , so we do not seek to improve it further — we use the same hypothesized upper bound  $D_{\mathbf{H}} \leq 10(n + m)$  to determine the iteration count (15). In Figure 6, we plot the errors  $\|\mathbf{X}_k - \mathbf{X}^*\|_2$  at each iteration against this heuristic and observe that it does indeed capture the convergence rate and provide an upper bound until errors saturate.

**3.5. Quadrature error analysis.** In this subsection, we discuss the inexactness of quadrature rules. These results can also be found in [5]. One assumption that was made in the preceding convergence analysis was that the coefficients  $\alpha_j$  in the  $p_j$ -series expansion of  $f$  were computed exactly. To relax this assumption, let

$$(17) \quad \rho_m(x) := \int_{\Gamma} \frac{f(z)}{z-x} dz - \sum_{j=1}^m \frac{f(z_j)}{z_j-x} w_j,$$

be a measure of the quadrature rule error. Denote the  $k$ th iteration of Algorithm 1, with the approximate coefficients, by

$$f_{k,m}(\mathbf{M}) := - \sum_{\ell=0}^{k-1} \left( \sum_{j=1}^m f(z_j) w_j \mathcal{C}_{\Sigma} [p_{\ell} w](z_j) \right) p_{\ell}(\mathbf{M}).$$

**Theorem 3.6.** *Under the assumptions of Lemma 3.2, let  $\mathbf{M}$  be a square matrix and suppose that*

$$\sum_{\ell=0}^{\infty} \varrho^{-\ell} \|p_{\ell}(\mathbf{M})\|_2 < \infty.$$

*Further suppose that  $\Gamma, f$  are as in Definition 2.2 and  $\{z_j\}_{j=1}^m, \{w_j\}_{j=1}^m$  are quadrature nodes and weights for  $\Gamma$ , respectively. Then, there exist  $\varepsilon_{m,\ell}$  satisfying  $|\varepsilon_{m,\ell}| \leq \|\rho_m\|_{\infty} := \max_{z \in \Sigma} |\rho_m(z)|$  and a constant  $C > 0$ , independent of  $f$ , such that*

$$\left\| f(\mathbf{M}) - f_{k,m}(\mathbf{M}) + \sum_{\ell=0}^{k-1} \varepsilon_{m,\ell} p_{\ell}(\mathbf{M}) \right\|_2 \leq CM \sum_{\ell=k}^{\infty} \varrho^{-\ell} \|p_{\ell}(\mathbf{M})\|_2.$$

In particular, following the proof of Theorem 3.5, Theorem 3.6 implies that when a generic  $\mathbf{M}$  is diagonalized as  $\mathbf{M} = \mathbf{V} \mathbf{\Lambda} \mathbf{V}^{-1}$  and satisfies  $\sigma(\mathbf{M}) \subset \Sigma$ , there exists some constant  $C' > 0$  such that

$$(18) \quad \|f(\mathbf{M}) - f_{k,m}(\mathbf{M})\|_2 \leq \|\mathbf{V}\|_2 \|\mathbf{V}^{-1}\|_2 \left( \|\rho_m\|_{\infty} \sum_{\ell=0}^{k-1} \|p_{\ell}(\mathbf{\Lambda})\|_2 + C' M \frac{\varrho^{-k}}{1 - \varrho^{-1}} \right).$$

Since  $\|p_{\ell}(\mathbf{M})\|_2 = O(1)$  when  $\mathbf{M}$  is generic and  $\sigma(\mathbf{M}) \subset \Sigma$ , the former term in the sum is likely to be small; however, as  $k$  increases, this term will eventually become large. See Appendix A for a discussion of why the errors still tend to remain small in this case. This appendix also contains convergence analysis for generic matrices whose eigenvalues may not lie in  $\Sigma$ .

**3.6. Complexity and timings.** To analyze the complexity of Algorithm 4, we assume that the numerical rank of  $c\varrho^{-k} \mathbf{J}_k \mathbf{K}_k$  is given by  $R(k)$  and that  $R(k) = 0$  for all  $k \geq k^*$  and some  $k^* \in \mathbb{N}$ . That is, we assume that the numerical rank of the weighted compression of  $\mathbf{J}_k \mathbf{K}_k$  is bounded and eventually becomes zero. This implies that the numerical rank of  $\mathbf{W}_k \mathbf{Z}_k$  is also bounded, and we denote this quantity by  $\hat{R}(k)$ . Suppose that  $T_{\mathbf{A}}$  is the cost of a left matrix-vector multiplication by  $\mathbf{A}$  and  $T_{\mathbf{B}}$  is the cost of a right matrix-vector multiplication by  $\mathbf{B}$ .

At the  $k$ th iteration of Algorithm 4, constructing the matrices  $\mathbf{V} p_k(\mathbf{A})$  and  $p_k(\mathbf{B}) \mathbf{U}$  requires at most

$$r(T_{\mathbf{A}} + T_{\mathbf{B}}) + 5r(m+n),$$

arithmetic operations. The construction of  $\mathbf{J}_k$  and  $\mathbf{K}_k$  requires at most

$$(2R(k-1) + R(k-2) + r)m + R(k-1)T_{\mathbf{A}},$$

arithmetic operations, and the construction of  $\mathbf{W}_{k+1}$  and  $\mathbf{Z}_{k+1}$  requires at most

$$(R(k) + r)m,$$

arithmetic operations. The compression of  $\mathbf{J}_k \mathbf{K}_k$  COMPRESS  $\left( \mathbf{J}_k, \mathbf{K}_k, \frac{\varrho^k \epsilon}{c} \right)$  requires

$$O\left( (2R(k-1) + R(k-2) + r)^3 + (2R(k-1) + R(k-2) + r)^2(m+n) \right),$$



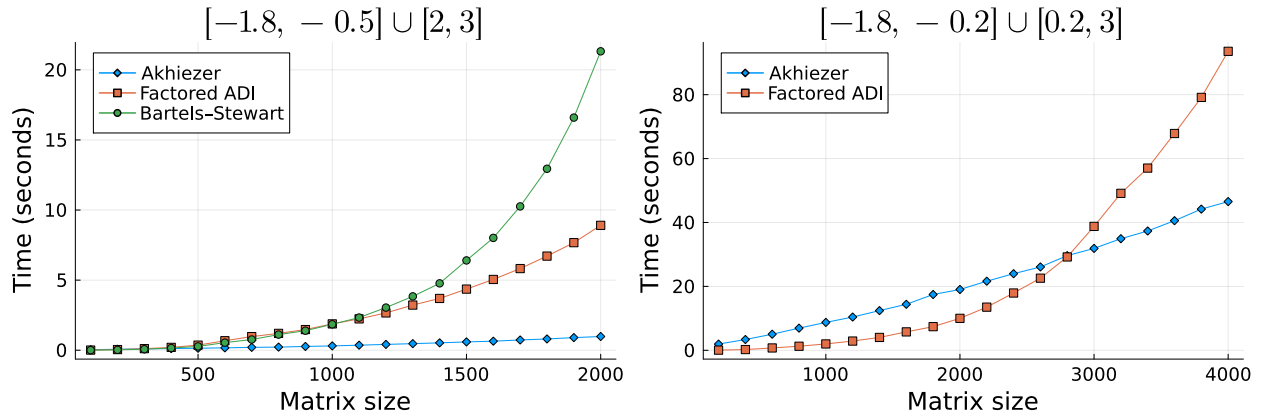


FIGURE 7. Timing comparisons of Algorithm 4 against the factored ADI and Bartels–Stewart algorithms for solving (1). Here, both factored ADI and Algorithm 4 are run with a tolerance of  $\epsilon = 10^{-14}$ ,  $\mathbf{A}$  and  $\mathbf{B}$  are both dense square matrices of varying size,  $\sigma(\mathbf{A}) \subset [2, 3]$  (left) and  $\sigma(\mathbf{A}) \subset [0.2, 3]$  (right),  $\mathbf{B} \subset [-1.8, -0.5]$  (left) and  $\mathbf{B} \subset [-1.8, -0.2]$  (right), and  $\mathbf{C}$  is rank 2. Bartels–Stewart is not included on the right, as its runtime is much longer than the other two methods. Note that the implementation of factored ADI could be sped up here by storing LU decompositions, but the Akhiezer iteration will still outperform it if  $m$  and  $n$  are sufficiently large.

arithmetic operations, while the compression of  $\mathbf{W}_k \mathbf{Z}_k$  `COMPRESS` ( $\mathbf{W}_k, \mathbf{Z}_k, \epsilon$ ) requires

$$O\left((R(k) + \hat{R}(k) + r)^3 + (R(k) + \hat{R}(k) + r)^2(m + n)\right),$$

arithmetic operations. Finally, the cost of computing the recurrence coefficients and  $p_j$ -series coefficients is assumed to be  $O(1)$  — computing the Akhiezer data requires  $O(k)$  operations for  $k$  iterations.

To bound the complexity of Algorithm 4 run for  $k$  iterations, denote

$$\mathcal{R} := \max_{j \in \mathbb{N}} \left\{ R(j), \hat{R}(j) \right\}.$$

Then, to run Algorithm 4 run for  $k$  iterations, we need

$$O\left(kr(T_{\mathbf{A}} + T_{\mathbf{B}}) + k\mathcal{R}T_{\mathbf{A}} + k(\mathcal{R} + r)^3 + k(\mathcal{R} + r)^2(m + n)\right),$$

arithmetic operations. Note that when the stopping criterion (15) is applied,  $k = O(\log(m + n))$ .

In the general case when  $T_{\mathbf{A}} = O(n^2)$ ,  $T_{\mathbf{B}} = O(m^2)$ ,  $r, \mathcal{R} \ll m, n$ , and the stopping criterion (15) is applied, Algorithm 4 requires<sup>4</sup>  $O(m^2 \log m + n^2 \log n)$  arithmetic operations. In contrast, the Bartels–Stewart algorithm requires  $O(m^3 + n^3)$  arithmetic operations [9]. Furthermore, methods such as Alternating-Directional-Implicit (ADI) iterations that require computing matrix inverses will also necessitate  $O(m^3 + n^3)$  arithmetic operations in general.

To demonstrate the advantageous complexity of our method, we include a timing comparison<sup>5</sup> of Algorithm 4 with factored ADI [15] and `sylvester`, the built-in Julia implementation of the Bartels–Stewart algorithm [9], in Figure 7. Even when the intervals of  $\Sigma$  are close, our method eventually outperforms its competitors as the size of  $\mathbf{X}$  increases.

<sup>4</sup>Note that  $O((m^2 + n^2) \log(m + n))$  is equivalent to  $O(m^2 \log m + n^2 \log n)$ .

<sup>5</sup>All computations in this paper are performed on a Lenovo laptop running Ubuntu version 20.04 with 8 cores and 16 GB of RAM with an Intel® Core™ i7-11800H processor running at 2.30 GHz.

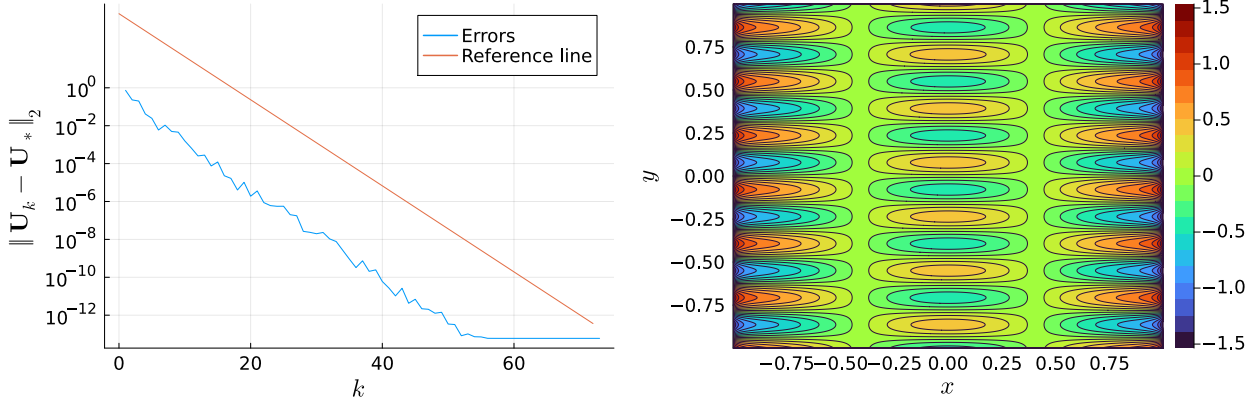


FIGURE 8. 2-norm error for  $\mathbf{U}_k$  against the true solution  $\mathbf{U}_*$  (computed via `sylvester` in Julia) at each iteration of Algorithm 4 in solving (20) (left) and corresponding approximate solution of (19) at  $n = 2000$  gridpoints with  $K_1(x, y) = K_2(x, y) = \exp(-2|x - y|)$ ,  $f_1(x) = \frac{\cos(4x)}{1.04 - x^2}$ , and  $g_1(x) = \sin(20x)$  (right). Here, the reference line denotes the convergence rate heuristic (16) with  $D_{\mathbf{H}}$  replaced by the hypothesized upper bound  $10(n + m)$ .

#### 4. EXAMPLES AND APPLICATIONS

**4.1. Integral equations.** Given Hölder continuous, symmetric kernels  $K_1, K_2 : [-1, 1]^2 \rightarrow \mathbb{R}$  and continuous functions  $f_1, \dots, f_r, g_1, \dots, g_r : [-1, 1] \rightarrow \mathbb{R}$ , we consider the integral equation

$$(19) \quad 2u(x, y) + \int_{-1}^1 K_1(x, x')u(x', y)dx' + \int_{-1}^1 K_2(y, y')u(x, y')dy' = \sum_{\ell=1}^r f_{\ell}(x)g_{\ell}(y),$$

for the unknown  $u : [-1, 1]^2 \rightarrow \mathbb{R}$ . We assume that the  $L^2([-1, 1])$  eigenvalues of the operators defined by  $K_1, K_2$  lie in the interval  $(-1 + \delta, \infty)$  for some  $\delta > 0$ . Denote the Gauss–Legendre quadrature nodes and weights for  $n$  sample points by  $\{x_j\}_{j=1}^n$  and  $\{w_j\}_{j=1}^n$ , respectively. Applying this quadrature rule to each integral in (19) and collocating at the points  $\{x_j\}_{j=1}^n$  in both  $x$  and  $y$  yields the Sylvester equation

$$(20) \quad (\mathbf{I} + \mathbf{K}_1)\mathbf{U} + \mathbf{U}(\mathbf{I} + \mathbf{K}_2) = \sum_{\ell=1}^r \mathbf{f}_{\ell}\mathbf{g}_{\ell}^T,$$

where  $\mathbf{K}_1, \mathbf{K}_2, \mathbf{U} \in \mathbb{R}^{n \times n}$  and  $\mathbf{f}_{\ell}, \mathbf{g}_{\ell} \in \mathbb{R}^n$  have entries

$$(21) \quad \begin{aligned} (\mathbf{K}_{1,2})_{j,k} &= \sqrt{w_j w_k} K_{1,2}(x_j, x_k), & \mathbf{U}_{j,k} &\approx \sqrt{w_j w_k} u(x_j, x_k), \\ (\mathbf{f}_{\ell})_j &= \sqrt{w_j} f_{\ell}(x_j), & (\mathbf{g}_{\ell})_j &= \sqrt{w_j} g_{\ell}(x_j), \quad \ell = 1, \dots, r. \end{aligned}$$

The eigenvalues of  $\mathbf{I} + \mathbf{K}_{1,2}$  are larger than  $\delta$  and less than<sup>6</sup>  $1 + \|\mathbf{K}_{1,2}\|_2$ , which remains bounded as  $n$  increases. Because  $\sum_{\ell=1}^r \mathbf{f}_{\ell}\mathbf{g}_{\ell}^T$  has rank at most  $r$ , the Akhiezer iteration can be applied as in Algorithm 4. The efficiency of our method allows for such integral equations to be solved on fine grids. In Figure 8, we plot both an approximate solution to (19) with  $K_1(x, y) = K_2(x, y) = \exp(-2|x - y|)$ ,  $r = 1$ ,  $f_1(x) = \frac{\cos(4x)}{1.04 - x^2}$ , and  $g_1(x) = \sin(20x)$  at  $n = 2000$  gridpoints and the error in (20) at each iteration of Algorithm 4.

<sup>6</sup>An upper bound can be more cheaply computed by instead using the Frobenius norm.

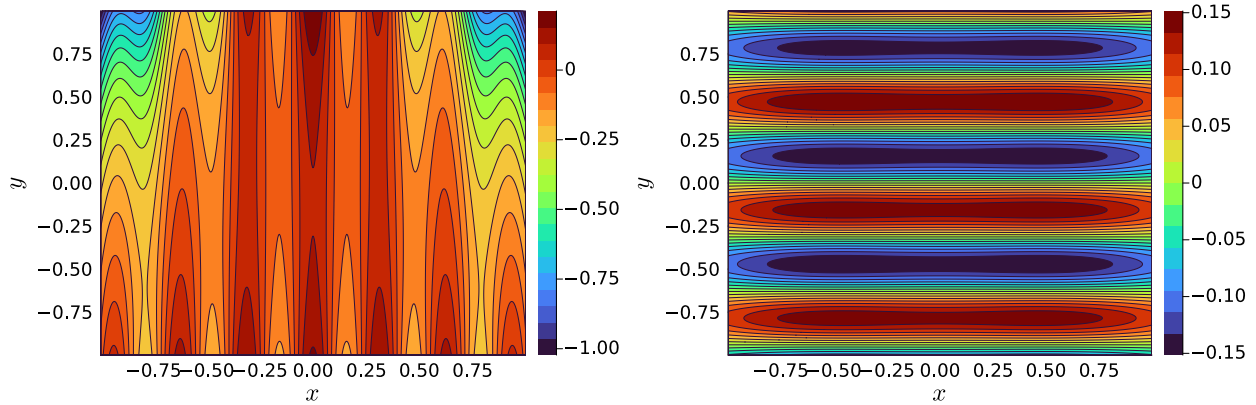


FIGURE 9. Approximate solution of (22) at  $n = 2000$  gridpoints with  $K_1(x, y) = K_2(x, y) = \exp(-2|x - y|)$ ,  $K_3(x, y) = \cos(20x) \exp(y)$ ,  $K_4(x, y) = \cosh(x) \sinh(y)$ ,  $f_1(x) = x^2$ , and  $g_1(x) = -\exp(x)$  (left) and  $K_1(x, y) = K_2(x, y) = \exp(-(x - y)^2)$ ,  $K_3(x, y) = y \operatorname{sech}^2(x)$ ,  $K_4(x, y) = \exp(x - y)$ ,  $f_1(x) = \frac{1}{x^4 + 2}$ , and  $g_1(x) = -\sin(10x)$  (right). In both cases, preconditioned GMRES applied to (23) converges in 1 iteration.

As an extension, given additional rank 1 kernel functions<sup>7</sup>  $K_3, K_4 : [-1, 1]^2 \rightarrow \mathbb{R}$ , consider the integral equation

$$(22) \quad \begin{aligned} 2u(x, y) + \int_{-1}^1 K_1(x, x')u(x', y)dx' + \int_{-1}^1 K_2(y, y')u(x, y')dy' \\ + \int_{-1}^1 \int_{-1}^1 K_3(x, x')u(x', y')K_4(y, y')dx'dy' = \sum_{\ell=1}^r f_\ell(x)g_\ell(y). \end{aligned}$$

Applying Gauss–Legendre quadrature to (22) in the same manner yields the generalized Sylvester equation

$$(23) \quad (\mathbf{I} + \mathbf{K}_1)\mathbf{U} + \mathbf{U}(\mathbf{I} + \mathbf{K}_2) + \mathbf{K}_3\mathbf{U}\mathbf{K}_4^T = \sum_{\ell=1}^r \mathbf{f}_\ell \mathbf{g}_\ell^T,$$

where  $\mathbf{K}_3, \mathbf{K}_4 \in \mathbb{R}^{n \times n}$  have entries

$$(\mathbf{K}_{3,4})_{j,k} = \sqrt{w_j w_k} K_{3,4}(x_j, x_k),$$

and the other matrices are defined as in (21). To see how Algorithm 4 can be used to solve (23), denote the solution to the Sylvester equation (1) by the linear map

$$T_{\mathbf{A}, \mathbf{B}}(\mathbf{C}) := \mathbf{X}.$$

Then, (23) is equivalent to the linear system

$$(24) \quad (\mathbf{I} + T_{(\mathbf{I} + \mathbf{K}_1), (\mathbf{I} + \mathbf{K}_2)}) (\mathbf{K}_3 \mathbf{U} \mathbf{K}_4^T) = T_{(\mathbf{I} + \mathbf{K}_1), (\mathbf{I} + \mathbf{K}_2)} \left( \sum_{\ell=1}^r \mathbf{f}_\ell \mathbf{g}_\ell^T \right).$$

Using Algorithm 4 to compute the action of  $T_{(\mathbf{I} + \mathbf{K}_1), (\mathbf{I} + \mathbf{K}_2)}$ , matrix-free GMRES or another iterative method can be used to solve (24). Furthermore, since this system is identity plus rank 1, GMRES will converge in at most two iterations. We include two solutions computed in this manner in Figure 9.

<sup>7</sup>This is a convenient but unnecessary assumption. To apply Algorithm 4 in the manner described, at least one of the resulting matrices  $\mathbf{K}_3$  and  $\mathbf{K}_4$  must be representable in low-rank form. In this case, the number of required GMRES iterations is one plus the rank of  $\mathbf{K}_4 \otimes \mathbf{K}_3$ .

**4.2. Collocation for the “good” Helmholtz equation.** Consider solving the inhomogeneous “good” Helmholtz equation on the square,

$$\begin{aligned} u_{xx}(x, y) + u_{yy}(x, y) - k^2 u(x, y) &= f(x, y), & (x, y) \in (-1, 1)^2, & \quad k \in \mathbb{R}, \\ u(\pm 1, y) &= 0, & y \in [-1, 1], \\ u(x, \pm 1) &= 0, & x \in [-1, 1]. \end{aligned}$$

We solve this problem not because the method developed will compete with the state-of-the-art solvers but to demonstrate three things: first, we show how a discretization can be produced that leads to a Sylvester matrix equation involving non-symmetric dense matrices with real eigenvalues. Second, we use this as an opportunity to highlight the kinds of challenges that arise in this method when discretizing operators with unbounded spectra. As we show, more work is needed to make the Akhiezer iteration practical in this setting. In particular, an effective preconditioner that preserves the real spectrum of operators is desirable and would potentially make the method very effective. Finally, we use the slow convergence rate of the algorithm in this setting to observe that our method exhibits remarkable stability, even when applied over thousands of iterations. Using an inverse-free, unpreconditioned method tests the limits of our approach. We note that in the case where  $k = 0$  (Poisson’s equation), several effective solvers already exist, including an optimal complexity spectral method based on ultraspherical polynomials and the ADI method [25].

To understand how to discretize this problem using collocation so that an appropriate Sylvester matrix equation is obtained, we consider the collocation discretization of a one-dimensional eigenvalue problem:

$$(25) \quad u''(x) = zu(x), \quad x \in (-1, 1), \quad u(\pm 1) = 0.$$

Let  $(p_j^{(\lambda)}(x))_{j=0}^{\infty}$  denote orthonormal ultraspherical polynomials with parameter  $\lambda$ , i.e., the orthonormal polynomials on  $[-1, 1]$  with respect to the normalized weight function  $Z_{\lambda}^{-1}(1-x^2)^{\lambda-1/2}$ . To keep notation a bit more classical, let  $(\check{T}_j(x))_{j=0}^{\infty}$  denote orthonormal Chebyshev polynomials of the first kind (ultraspherical,  $\lambda = 0$ ) with respect to the normalized weight function  $\pi^{-1}(1-x^2)^{-1/2}$  on  $[-1, 1]$ . We follow the approach in [59]. From [45], for example, there exists a strictly upper-triangular, sparse  $N \times N$  matrix  $\mathbf{D}_2$  such that if

$$\begin{aligned} v(x) &= \sum_{j=0}^{N-1} v_j \check{T}_j(x), & \mathbf{v} &= (v_0, \dots, v_{N-1})^T, \\ \mathbf{w} &= (w_0, \dots, w_{N-1})^T, & \mathbf{w} &= \mathbf{D}_2 \mathbf{v}, \end{aligned}$$

then

$$v''(x) = \sum_{j=0}^{N-1} w_j p_j^{(2)}(x).$$

Now, for a grid of  $M$  points  $-1 < x_1 < x_2 < \dots < x_M < 1$ ,  $x_j = x_j(M)$ , define the  $M \times N$  matrix,

$$\mathbf{E}_M(\lambda) = (p_j^{(\lambda)}(x_i))_{\substack{1 \leq i \leq M \\ 0 \leq j \leq N-1}},$$

and define the boundary operator

$$\mathbf{B} = \begin{pmatrix} \check{T}_0(1) & \check{T}_1(1) & \cdots & \check{T}_{N-1}(1) \\ \check{T}_0(-1) & \check{T}_1(-1) & \cdots & \check{T}_{N-1}(-1) \end{pmatrix}.$$

The discretization of the problem (25) is then given by the generalized eigenvalue problem

$$\begin{pmatrix} \mathbf{B} \\ \mathbf{E}_{N-2}(2)\mathbf{D}_2 \end{pmatrix} \mathbf{u} = z \begin{pmatrix} \mathbf{0} \\ \mathbf{E}_{N-2}(0) \end{pmatrix} \mathbf{u}.$$

To write this as a conventional eigenvalue problem, we let<sup>8</sup>

$$\mathbf{Q}, \mathbf{R} = \text{qr}(\mathbf{B}^T), \quad \mathbf{T} = \mathbf{Q}_{:,3:N},$$

so that the columns of  $\mathbf{T}$  form a basis for the nullspace of  $\mathbf{B}$ . Then, in writing  $\mathbf{u} = \mathbf{T}\mathbf{v}$ , we find the eigenvalue problem<sup>9</sup>

$$\mathbf{E}_{N-2}(2)\mathbf{D}_2\mathbf{T}\mathbf{v} = z\mathbf{E}_{N-2}(0)\mathbf{T}\mathbf{v} \quad \Rightarrow \quad (\mathbf{E}_{N-2}(0)\mathbf{T})^{-1}\mathbf{E}_{N-2}(2)\mathbf{D}_2\mathbf{T}\mathbf{v} = z\mathbf{v}.$$

Then, define

$$\mathbf{A}_N = (\mathbf{E}_{N-2}(0)\mathbf{T})^{-1}\mathbf{E}_{N-2}(2)\mathbf{D}_2\mathbf{T}.$$

Empirically, and surprisingly, we see that  $\mathbf{A}_N$  has negative eigenvalues.

We approximate

$$u(x, y) \approx u_N(x, y) = \sum_{j=0}^{N-1} \sum_{i=0}^{N-1} u_{ij} \check{T}_j(x) \check{T}_i(y),$$

and see that the discretization of the “good” Helmholtz equation is then given by

$$(26) \quad \mathbf{A}_N \mathbf{Y} + \mathbf{Y} \mathbf{A}_N^T - k^2 \mathbf{Y} = \mathbf{G}, \quad \mathbf{X} = \mathbf{T} \mathbf{Y} \mathbf{T}^T, \quad \mathbf{X} = (u_{ij})_{\substack{1 \leq i \leq N, \\ 1 \leq j \leq N}},$$

$$\mathbf{G} = (\mathbf{E}_{N-2}(0)\mathbf{T})^{-1} \mathbf{F} (\mathbf{E}_{N-2}(0)\mathbf{T})^{-T}, \quad \mathbf{F} = (f(x_i, x_j))_{\substack{1 \leq i \leq N-2, \\ 1 \leq j \leq N-2}}.$$

The success of the above approach is limited due to the fact that the Laplacian is unbounded and the eigenvalues of  $\mathbf{A}_N$  grow rapidly as  $N$  increases. As a consequence of this, the approximation of the series coefficients  $\alpha_j$  via circular contours around each interval of  $\Sigma = \Sigma_N$  requires an increasing number of quadrature points as  $N$  increases. The latter issue can be partially addressed using the principal value integral

$$-\frac{1}{\pi i} \oint_{-i\infty}^{i\infty} \frac{dz}{z-x} = \text{sign}(x), \quad x \in \mathbb{C} \setminus i\mathbb{R},$$

so that the series coefficients are given by

$$\alpha_j = \frac{1}{2\pi i} \int_{\Sigma} \left( 2 \oint_{i\infty}^{-i\infty} \frac{dz}{z-x} \right) p_j(x) w(x) dx.$$

Following [33, Section 7.1], the change of variables  $y = \frac{2}{\pi} \arctan(iz)$  yields

$$\alpha_j = \frac{1}{2\pi i} \int_{\Sigma} \left( i\pi \int_{-1}^1 \frac{\sec^2(\frac{\pi}{2}y)}{x + i \tan(\frac{\pi}{2}y)} dy \right) p_j(x) w(x) dx.$$

Denote the Gauss-Legendre quadrature nodes and weights by  $\{y_\ell\}_{\ell=1}^m$  and  $\{w_\ell\}_{\ell=1}^m$ , respectively. Then,

$$\alpha_j \approx i\pi \sum_{\ell=1}^m (z_\ell^2 + 1) w_\ell \mathcal{C}_\Sigma [p_j w](-iz_\ell), \quad z_\ell = \tan\left(\frac{\pi y_\ell}{2}\right).$$

Empirically, we find that this requires fewer quadrature points to obtain an accurate approximation to the series coefficients  $\alpha_j$  when the eigenvalues of  $\mathbf{A}_N$  are large<sup>10</sup>. In Figures 10 and 11, we plot approximate solutions obtained in this manner as well as the error at each iteration in solving (26). As expected, our method requires many iterations even when  $N$  is small, but we are able to generate approximate solutions nonetheless.

<sup>8</sup>We note that it is possible to use a different choice for  $\mathbf{T}$  that is sparse, but we do not need this here.

<sup>9</sup>Note that the invertibility of  $\mathbf{E}_{N-2}(0)\mathbf{T}$  follows from the fact that the only polynomial of degree  $N$  that interpolates zero at the union of the nodes and  $\{1, -1\}$  is the trivial one.

<sup>10</sup>In fact, this approach seems to require fewer quadrature points in most cases, even when the intervals of  $\Sigma$  are small and well-separated. When 0 does not lie in the gap between intervals, these formulae will need to be shifted appropriately.

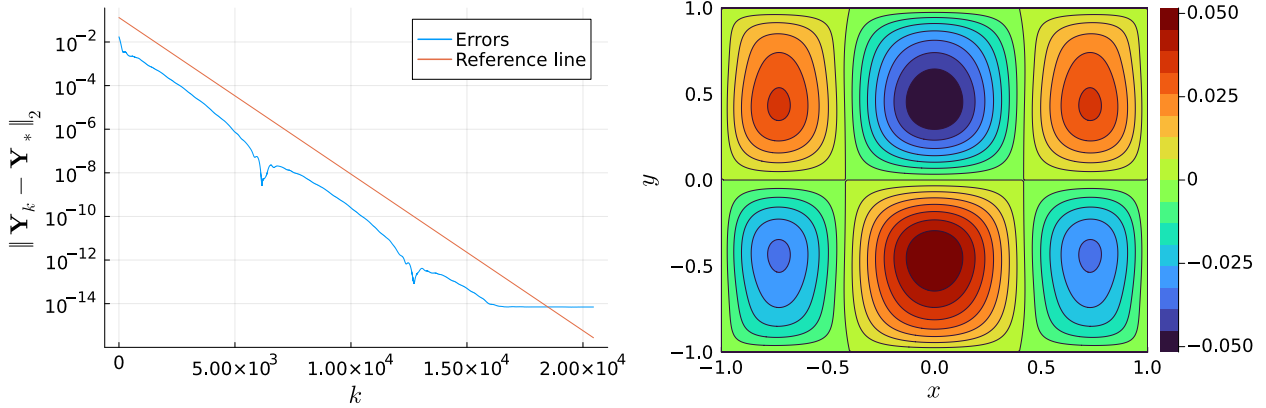


FIGURE 10. 2-norm error for  $\mathbf{Y}_k$  against the true solution  $\mathbf{Y}_*$  (computed via `sylvester` in Julia) at each iteration of Algorithm 4 in solving (26) (left) and corresponding  $N = 10$  approximate solution of Poisson’s equation ( $k = 0$ ) with  $f(x, y) = \cos(4x) \text{sign}(y)$  (right). Here, the reference line denotes the convergence rate heuristic (16) with  $D_{\mathbf{H}}$  replaced by the hypothesized upper bound  $10(n + m)$ .

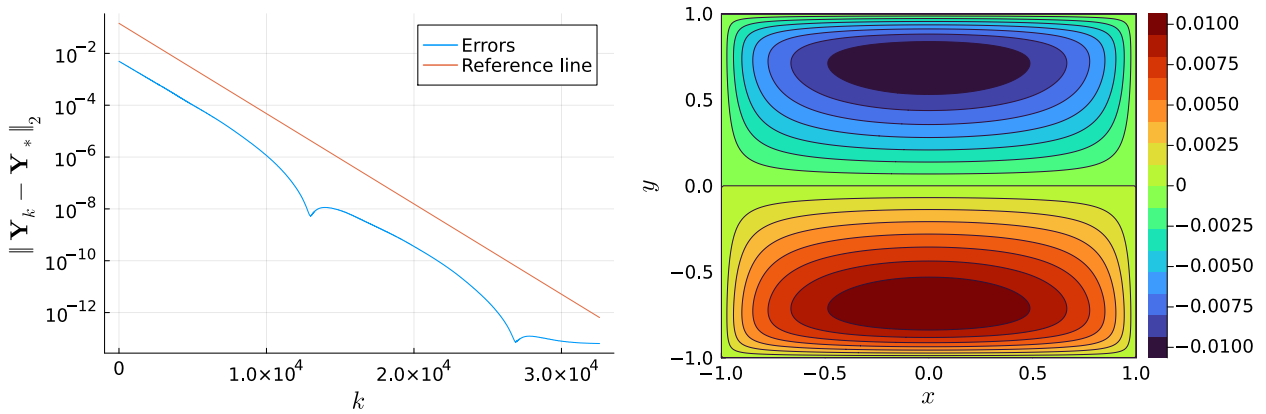


FIGURE 11. 2-norm error for  $\mathbf{Y}_k$  against the true solution  $\mathbf{Y}_*$  (computed via `sylvester` in Julia) at each iteration of Algorithm 4 in solving (26) (left) and corresponding  $N = 20$  approximate solution of the “good” Helmholtz equation with  $f(x, y) = \cos(x) \sin(y)$  and  $k = 7$  (right). Here, the reference line denotes the convergence rate heuristic (16) with  $D_{\mathbf{H}}$  replaced by the hypothesized upper bound  $10(n + m)$ .

While poor conditioning and the small problem size mean that our method is uncompetitive with direct solvers such as the Bartels–Stewart algorithm for this task, this application demonstrates the behavior of our Sylvester equation solver applied to ill-conditioned problems. Even in these settings where the eigenvalues are large, we observe that our method appears stable and converges at the rate given by our analysis.

## 5. OTHER APPLICATIONS

**5.1. Algebraic Riccati equations.** An algebraic Riccati equation is a generalization of the Sylvester equation of the form

$$(27) \quad \mathbf{A}\mathbf{X} - \mathbf{X}\mathbf{B} - \mathbf{X}\mathbf{D}\mathbf{X} = \mathbf{C}.$$

Under certain conditions on the data matrices, a solution to (27) can be obtained by computing the sign of the matrix [18]

$$\mathbf{H} = \begin{pmatrix} \mathbf{A} & \mathbf{D} \\ \mathbf{C} & \mathbf{B} \end{pmatrix}.$$

If the eigenvalues of  $\mathbf{H}$  are known to lie on or near a collection of disjoint intervals  $\Sigma$ , solving the Ricatti equation (27) is a direct application of the Akhiezer iteration, albeit without the decoupled and low-rank structure of the Sylvester equation algorithms. However, if only the eigenvalues of the individual data matrices are known, little can be said in general about the eigenvalues of  $\mathbf{H}$ . Particular cases when the eigenvalues of  $\mathbf{H}$  are easily determined are when  $\mathbf{C} = \mathbf{0}$  and when  $\mathbf{D} = \mathbf{0}$ . The latter case reduces precisely to the Sylvester equation (1). The former case has the trivial solution  $\mathbf{X} = \mathbf{0}$ . If an invertible solution  $\mathbf{X}$  exists, (27) is equivalent to

$$\mathbf{X}^{-1}\mathbf{A} - \mathbf{B}\mathbf{X}^{-1} - \mathbf{D} = 0,$$

which is simply a Sylvester equation for  $\mathbf{X}^{-1}$ . Thus, while our method can, in principle, be generalized to algebraic Ricatti equations, knowledge of the eigenvalues of the full block matrix  $\mathbf{H}$  is required to compute anything nontrivial. If the eigenvalues of  $\mathbf{H}$  are suspected to lie on a collection of disjoint intervals, the adaptive procedure described in [5, Section 5] could be employed to approximate these intervals, then the Akhiezer iteration could be applied directly to compute  $\text{sign}(\mathbf{H})$  and solve (27).

**5.2. Fréchet derivatives.** A natural application of this work is to the computation of Fréchet derivatives. Given a matrix  $\mathbf{A} \in \mathbb{C}^{n \times n}$  and matrix function  $f : \mathbb{C}^{n \times n} \rightarrow \mathbb{C}^{n \times n}$ , the Fréchet derivative of  $f$  at  $\mathbf{A}$  is a linear map  $L_f(\mathbf{A}, \diamond)$  satisfying

$$f(\mathbf{A} + \mathbf{E}) - f(\mathbf{A}) - L_f(\mathbf{A}, \mathbf{E}) = o(\|\mathbf{E}\|),$$

for all  $\mathbf{E} \in \mathbb{C}^{n \times n}$ . Fréchet derivatives need not exist, but must be unique if they do [31, Section 3.1]. By modifying [41, Theorem 2.1] and its proof to use lower triangular matrices, if  $p$  denotes the size of the largest Jordan block of  $\mathbf{A}$  and  $f$  is  $2p - 1$  times continuously differentiable on an open set containing the spectrum of  $\mathbf{A}$ , then for any  $\mathbf{E} \in \mathbb{C}^{n \times n}$ ,

$$f \begin{pmatrix} \mathbf{A} & \mathbf{0} \\ \mathbf{E} & \mathbf{A} \end{pmatrix} = \begin{pmatrix} f(\mathbf{A}) & \mathbf{0} \\ L_f(\mathbf{A}, \mathbf{E}) & f(\mathbf{A}) \end{pmatrix}.$$

Since computing the Fréchet derivative requires only the lower left block of this matrix function, the recurrences utilized in Algorithms 2 and 4 can be applied nearly directly with  $f$  in place of the sign function; only the series coefficients  $\alpha_j$  need be modified appropriately. In Figure 12, we plot the error at each iteration of computing the Fréchet derivative for the matrix sign function and matrix exponential. We observe that the method converges quickly with the same convergence guarantees as when it is applied to Sylvester equations. The Fréchet derivative of the matrix sign function is useful for analyzing the stability of algorithms to compute the matrix sign, matrix square root, and other related matrix functions [34].

**5.3. Matrix square roots and the polar decomposition.** The matrix sign function can also be used to compute the matrix square root and inverse square root. In particular, if  $\mathbf{A} \in \mathbb{C}^{n \times n}$  has no eigenvalues on  $(-\infty, 0]$ , then [31, Equation 6.32]

$$\text{sign} \begin{pmatrix} 0 & \mathbf{A} \\ \mathbf{I} & 0 \end{pmatrix} = \begin{pmatrix} 0 & \mathbf{A}^{1/2} \\ \mathbf{A}^{-1/2} & 0 \end{pmatrix}.$$

If  $\mathbf{A}$  has eigenvalues contained in or near some interval  $[a, b]$  on the positive real axis, the eigenvalues of  $\begin{pmatrix} 0 & \mathbf{A} \\ \mathbf{I} & 0 \end{pmatrix}$  are in or near  $[-\sqrt{b}, -\sqrt{a}] \cup [\sqrt{a}, \sqrt{b}]$ , and the Akhiezer iteration can be applied to compute  $\mathbf{A}^{1/2}$  and  $\mathbf{A}^{-1/2}$  in parallel. The off-diagonal structure of the relevant block matrix prevents the direct application of Lemma 3.1, and an analogous result for off-diagonal block  $2 \times 2$  matrices would need to be worked out for this approach to be made efficient. It is currently unclear

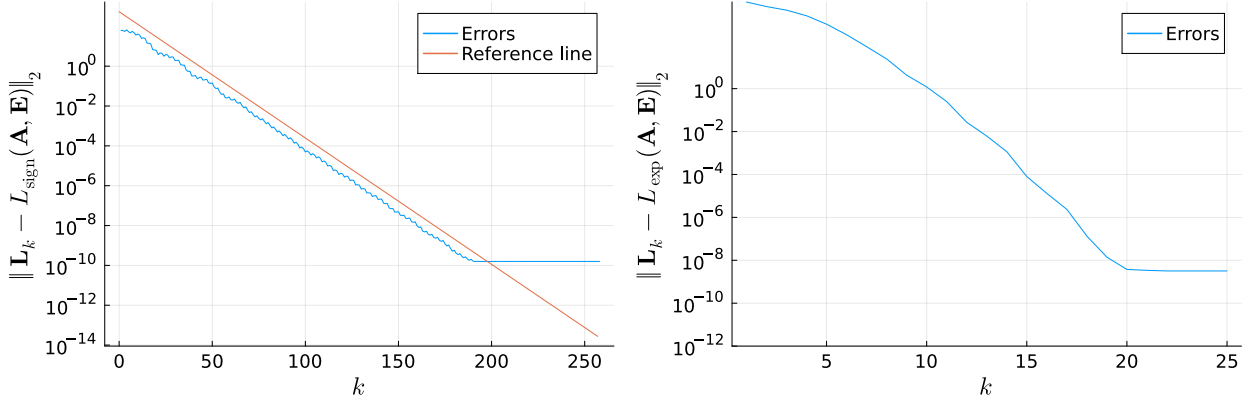


FIGURE 12. 2-norm error for approximation  $\mathbf{L}_k$  to  $L_f(\mathbf{A}, \mathbf{E})$  at each iteration of Algorithm 4 modified to compute Fréchet derivatives for  $f(x) = \text{sign}(x)$  (left) and  $f(x) = \exp(x)$  (right). Here,  $\mathbf{A} \in \mathbb{R}^{200 \times 200}$  has eigenvalues in  $[-2, -0.5] \cup [0.5, 6]$  and  $\mathbf{E}$  is rank 4. Because the exponential function is entire, our algorithm achieves superexponential convergence before errors saturate. The true solution is computed via the Newton iteration [2, Section 5] (left) and the built-in `Julia` function `exp` applied to  $\begin{pmatrix} \mathbf{A} & \mathbf{0} \\ \mathbf{E} & \mathbf{A} \end{pmatrix}$  (right). Here, the reference line denotes the convergence rate bound (14) with  $D_{\mathbf{M}}$  replaced by the hypothesized upper bound  $10\ell$  for generic  $\mathbf{M} \in \mathbb{C}^{\ell \times \ell}$ .

whether this would be more efficient than directly applying the Akhiezer iteration to  $\mathbf{A}$  to compute  $\mathbf{A}^{1/2}$  and  $\mathbf{A}^{-1/2}$  separately. Regardless, the Akhiezer iteration should produce an inverse-free method for computing the matrix square root and inverse square root; we leave this for future work.

Similarly, the matrix sign function is connected to the polar decomposition, which can be used to solve the orthogonal Procrustes problem [31, Theorem 8.6a]. If the polar decomposition of a matrix  $\mathbf{A} \in \mathbb{C}^{m \times n}$  ( $m \geq n$ ) is given by  $\mathbf{A} = \mathbf{U}\mathbf{H}$  where  $\mathbf{U} \in \mathbb{C}^{m \times n}$  has orthonormal columns and  $\mathbf{H} \in \mathbb{C}^{n \times n}$  is Hermitian and positive semidefinite, then [31, Equation 8.6]

$$\text{sign} \begin{pmatrix} 0 & \mathbf{A} \\ \mathbf{A}^* & 0 \end{pmatrix} = \begin{pmatrix} 0 & \mathbf{U} \\ \mathbf{U}^* & 0 \end{pmatrix}.$$

Thus, the Akhiezer iteration can be applied to compute the polar factor  $\mathbf{U}$  of the polar decomposition, in particular when the eigenvalues of  $\mathbf{A}^*\mathbf{A}$  are located in or near a known interval on the real axis. In the special case where  $\mathbf{A}$  is symmetric, an algorithm is immediate as  $\text{sign}(\mathbf{A}) = \mathbf{U}$ . Otherwise, an off-diagonal analog to Lemma 3.1 would likely be necessary for this approach to be made efficient. Another option is to compute the polar factor by applying the Akhiezer iteration to the inverse square root with the formula  $\mathbf{U} = \mathbf{A}(\mathbf{A}^*\mathbf{A})^{-1/2}$  [32, Chapter 8].

The Fréchet derivative of the polar decomposition can be obtained via the identity [28]

$$\text{sign} \begin{pmatrix} 0 & \mathbf{A} & 0 & \mathbf{E} \\ \mathbf{A}^* & 0 & \mathbf{E}^* & 0 \\ 0 & 0 & 0 & \mathbf{A} \\ 0 & 0 & \mathbf{A}^* & 0 \end{pmatrix} = \begin{pmatrix} 0 & \mathcal{P}(\mathbf{A}) & 0 & L_{\mathcal{P}}(\mathbf{A}, \mathbf{E}) \\ \mathcal{P}(\mathbf{A})^* & 0 & L_{\mathcal{P}}(\mathbf{A}, \mathbf{E})^* & 0 \\ 0 & 0 & 0 & \mathcal{P}(\mathbf{A}) \\ 0 & 0 & \mathcal{P}(\mathbf{A})^* & 0 \end{pmatrix}.$$

Here,  $\mathcal{P}$  denotes a function that maps a matrix to its polar factor and  $\mathbf{A}, \mathbf{E} \in \mathbb{C}^{n \times n}$ . The Akhiezer iteration can again be applied to compute  $L_{\mathcal{P}}(\mathbf{A}, \mathbf{E})$ , in particular when the eigenvalues  $\mathbf{A}^*\mathbf{A}$  are located in or near a known interval on the real axis since the eigenvalues of the relevant block matrix are given by both square roots of these eigenvalues. Once again, an analog of Lemma 3.1



for  $4 \times 4$  block matrices with the relevant sparsity pattern is likely needed for efficiency, but this would yield an inverse-free method that, in contrast with that of [28], would not require that all singular values of  $\mathbf{A}$  be small.

## 6. DISCUSSION AND FUTURE WORK

Perhaps the largest question that we have not addressed is that of adaptivity. Throughout this work, we have assumed access to intervals on the real axis that (approximately) contain the spectra of the coefficient matrices  $\mathbf{A}$  and  $\mathbf{B}$ . If these intervals are instead unknown, the approach outlined in [5, Section 5] can be applied to the block matrix  $\mathbf{H}$  from (10) to approximate the necessary intervals. Alternatively, since the problem of finding the eigenvalues of  $\mathbf{H}$  decouples, the same method with a single interval and shifted and scaled Chebyshev polynomials could be applied to each coefficient matrix individually. In the low-rank case of Algorithm 4, one could also consider performing this analysis with the norms of the iterates  $\mathbf{J}_k, \mathbf{K}_k$  as empirically, these appear to grow at the same rate as the norm of  $\mathbf{H}$ .

A more difficult generalization would be allowing the coefficient matrices to have nonreal eigenvalues. For instance,  $\mathbf{A}$  and  $\mathbf{B}$  could have eigenvalues contained in disjoint open sets in the complex plane. If these sets are well-separated, there potentially exists a pair of intervals on the real axis, or a pair of lines in the complex plane, that enable our method to converge in a reasonable number of iterations. Such a result exists for the related Chebyshev iteration and relies on the notion of an “optimal ellipse” [38, 39]. Extending this notion to higher genus cut domains is a challenging open problem. Solving it likely requires a complete understanding of the generalized Bernstein ellipses of Figure 2. Such a generalization could, for instance, enable an inverse-free method for the matrix-sign approach to eigenvalue computation when used in place of the Newton iteration in [8, Section 4].

For symmetric matrices,  $\text{sign}(\mathbf{M})$  is equal to the polar factor for  $\mathbf{M}$ . The Akhiezer polynomials could be applied in the context of divide-and-conquer eigensolvers based on spectral projections attained via the polar factor [43]. An inverse-free polar decomposition method based on Halley’s iteration was developed in [42], where inverse factors are rewritten using QR decompositions of a block matrix related to the iterate. However, the Akhiezer polynomials should lead to an eigensolver with the polar factorization step only requiring matrix products.

We have not attempted to implement methods involving hierarchical numerical linear algebra, but a natural connection to consider is the setting where  $\mathbf{A}$ ,  $\mathbf{B}$  and  $\mathbf{C}$  are rank-structured. As shown in [35], it is often the case that  $\mathbf{X}$  is well-approximated in this setting by a rank-structured matrix. Combining the Akhiezer iteration with the divide-and-conquer scheme in [35] would take advantage of fast multipole-based matrix-vector products available for  $\mathbf{A}$  and  $\mathbf{B}$  and potentially supply an inverse-free version of the algorithms.

## ACKNOWLEDGMENTS

We thank Mikaël Slevinsky and Sheehan Olver for valuable discussions. This work was supported in part by the National Science Foundation under DMS-2306438 (TT) and DMS-2410045 (HW).

## APPENDIX A. ADDITIONAL CONSIDERATIONS

In this section, we first discuss matrices that have complex eigenvalues and then discuss truncation errors from the approximation of contour integrals.

**A.1. Complex eigenvalues.** A particular class of generic matrices that one may wish to consider applying our methods to are matrices whose eigenvalues lie near, but not exactly on  $\Sigma$ . All theorems in [5] apply to this class. We include some of these results here without proof.

The primary difference between eigenvalues on  $\Sigma$  and eigenvalues near  $\Sigma$  is that the convergence rate of our algorithms now depends on the “worst offender” eigenvalue of the generic matrix  $\mathbf{M}$ , as

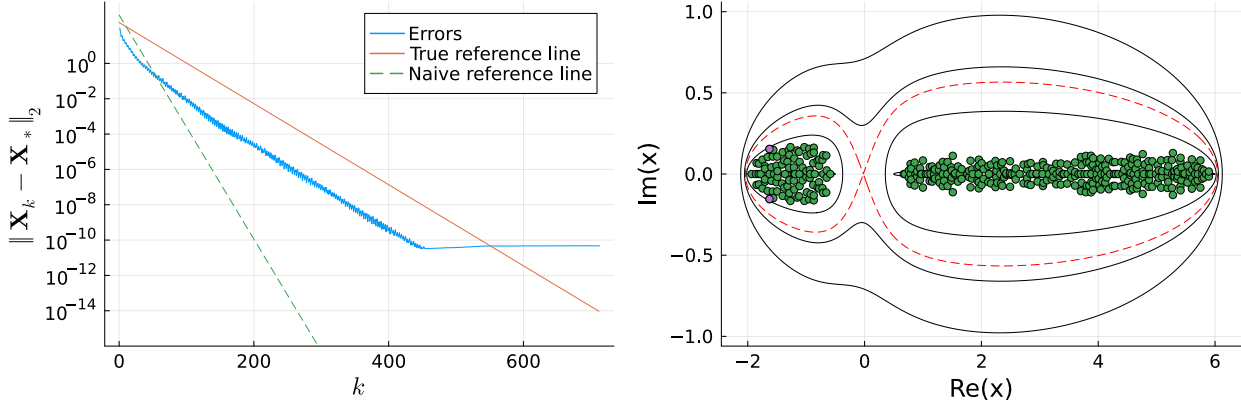


FIGURE 13. 2-norm error in solving (1) for  $\mathbf{X}_k$  against the true solution  $\mathbf{X}_*$  (computed via `sylvester` in Julia) at each iteration plotted against the convergence rate heuristic (16) (with  $D_{\mathbf{H}}$  replaced by the hypothesized upper bound  $10(n+m)$ ) corresponding to  $\varrho$  (dashed green line) and  $\varrho_{\mathbf{H}}$  (orange line) where  $\mathbf{A} \in \mathbb{R}^{300 \times 300}$  has eigenvalues near  $[0.5, 6]$ ,  $\mathbf{B} \in \mathbb{R}^{100 \times 100}$  has eigenvalues near  $[-2, -0.5]$ , and  $\mathbf{C}$  is rank 2 (left) and eigenvalues of  $\mathbf{H}$  superimposed over the generalized Bernstein ellipses of Figure 2 with the “worst offender” colored in purple (right). Since all eigenvalues are contained within the red dashed level curve, the method still converges.

measured by  $\text{Re } \mathfrak{g}$ . Specifically, the convergence rate of Algorithm 1 is governed by the function

$$\nu(z; \mathbf{M}) = \max_{\lambda \in \sigma(\mathbf{M})} \text{Re } \mathfrak{g}(\lambda) - \text{Re } \mathfrak{g}(z).$$

In this setting, the conclusion of Theorem 3.5 is modified to be

$$(28) \quad \|f(\mathbf{M}) - \mathbf{F}_k\|_2 \leq C' M \|\mathbf{V}\|_2 \|\mathbf{V}^{-1}\|_2 \frac{e^{k\nu(z_*; \mathbf{M})}}{1 - e^{\nu(z_*; \mathbf{M})}},$$

where  $z_*$  is any point on the level curve  $\Gamma_{\varrho} = \partial B_{\varrho}$  (13), interior to which  $f$  is analytic. See Lemma 3.2.

When  $f$  is the sign function, this implies that there exists some constant  $D_{\mathbf{M}} > 0$  such that

$$\|\text{sign}(\mathbf{M}) - \mathbf{F}_k\|_2 \leq D_{\mathbf{M}} \frac{e^{k\nu(z_*; \mathbf{M})}}{1 - e^{\nu(z_*; \mathbf{M})}}.$$

Applying the hypothesized bound  $D_{\mathbf{M}} \leq 10\ell$  of Section 3.4 for generic  $\mathbf{M} \in \mathbb{C}^{\ell \times \ell}$ , given a tolerance  $\epsilon > 0$  and denoting  $\varrho_{\mathbf{M}} = e^{\nu(z_*; \mathbf{M})}$ , we require

$$k = \left\lceil -\log_{\varrho_{\mathbf{H}}} \frac{\epsilon(1 - \varrho_{\mathbf{H}}^{-1})}{5(n+m)} \right\rceil,$$

iterations to ensure that the iterate  $\mathbf{X}_k$  of our method (Algorithms 2 or 4) satisfies

$$\|\mathbf{X}_k - \mathbf{X}_*\|_2 \leq \epsilon,$$

where  $\mathbf{X}_*$  denotes the solution of the Sylvester equation (1). In Figure 13, we plot the convergence of Algorithm 4 applied to coefficient matrices  $\mathbf{A}$  and  $\mathbf{B}$  with eigenvalues near  $[0.5, 6]$  and  $[-2, -0.5]$ , respectively. The iteration converges to the solution  $\mathbf{X}_*$  at the slower rate  $\varrho_{\mathbf{H}}^{-1}$  governed by the “worst offender” eigenvalue.

**A.2. Further quadrature error analysis.** To incorporate errors from quadrature rules in the context of Algorithm 1, the estimate (28) can be inserted into (18). For an additional estimate, we recall (17) and restate [5, Theorem 4.9].

**Theorem A.1.** Let  $\Sigma = \bigcup_{j=1}^{g+1} [\beta_j, \gamma_j] \subset \mathbb{R}$  be a union of disjoint intervals and  $w$  be a weight function of the form (9) and denote the corresponding orthonormal polynomials by  $(p_j(x))_{j=0}^{\infty}$ . Suppose that  $\Gamma, f$  are as in Definition 2.2 and  $\{z_j\}_{j=1}^m, \{w_j\}_{j=1}^m$  are quadrature nodes and weights for  $\Gamma$ , respectively. Suppose further that  $\mathbf{M} \in \mathbb{C}^{n \times n}$  is generic and satisfies  $\nu(z_j; \mathbf{M}) < 0$  for  $j = 1, 2, \dots, m$ ,  $|f(z)| \leq M$  for  $z \in \Gamma$ , and  $\sum_{j=1}^m |w_j| \leq 2\pi L$ . Then, there exists  $c' > 0$  such that

$$\|f(\mathbf{M}) - f_{k,m}(\mathbf{M})\|_2 \leq \|\mathbf{V}\|_2 \|\mathbf{V}^{-1}\|_2 \left( \frac{1}{2\pi} \max_{\lambda \in \sigma(\mathbf{M})} |\rho_m(\lambda)| + c'LM \max_{j \in \{1, \dots, m\}} \frac{e^{k\nu(z_j; \mathbf{M})}}{1 - e^{\nu(z_j; \mathbf{M})}} \right),$$

where  $\mathbf{M}$  is diagonalized as  $\mathbf{M} = \mathbf{V}\mathbf{\Lambda}\mathbf{V}^{-1}$ .

Define

$$\nu(\mathbf{M}) = \max_{\lambda \in \sigma(\mathbf{M})} \operatorname{Re} \mathbf{g}(\lambda).$$

Supposing that  $\Gamma \subset B_\varrho$ , combining (28) with Theorem A.1 yields that

$$\begin{aligned} \frac{\|f(\mathbf{M}) - f_{k,m}(\mathbf{M})\|_2}{\|\mathbf{V}\|_2 \|\mathbf{V}^{-1}\|_2} &\leq \min \left\{ \|\rho_m\|_\infty \sum_{\ell=0}^{k-1} \|p_\ell(\mathbf{\Lambda})\|_2 + C'M \frac{e^{k\nu(z_*; \mathbf{M})}}{1 - e^{\nu(z_*; \mathbf{M})}}, \right. \\ &\quad \left. \frac{1}{2\pi} \|\rho_m(\mathbf{\Lambda})\|_2 + c'LM \max_{j \in \{1, \dots, m\}} \frac{e^{k\nu(z_j; \mathbf{M})}}{1 - e^{\nu(z_j; \mathbf{M})}} \right\} \\ &\leq \min \left\{ d \|\rho_m\|_\infty \sum_{\ell=0}^{k-1} e^{\ell\nu(\mathbf{M})} + C'M \frac{e^{k\nu(z_*; \mathbf{M})}}{1 - e^{\nu(z_*; \mathbf{M})}}, \right. \\ &\quad \left. \frac{1}{2\pi} \|\rho_m(\mathbf{\Lambda})\|_2 + c'LM \max_{j \in \{1, \dots, m\}} \frac{e^{k\nu(z_j; \mathbf{M})}}{1 - e^{\nu(z_j; \mathbf{M})}} \right\}, \end{aligned}$$

for some constant  $d > 0$ .

Empirically, we find that the first term in the minimum typically gives a tighter bound; however, the latter term reflects that errors remain small as the iteration proceeds and  $\sum_{\ell=0}^{k-1} \|p_\ell(\mathbf{\Lambda})\|_2$  becomes large. Furthermore, if the eigenvalues of  $\mathbf{M}$  are not contained in  $\Sigma$ , the latter term will still be small, giving useful bounds. The first term will also likely be small, but as  $\nu(\mathbf{M}) > 0$ , the sum grows exponentially with respect to  $k$ . In this case, the balance, i.e., which term gives a better bound in a given situation, will change.

## REFERENCES

- [1] N. I. Akhiezer. *Elements of the Theory of Elliptic Functions*, volume 79 of *Translations of Mathematical Monographs*. American Mathematical Society, 1970.
- [2] A. H. Al-Mohy and N. J. Higham. The complex step approximation to the Fréchet derivative of a matrix function. *Numerical Algorithms*, 53(1):133–148, 2009.
- [3] A. C. Antoulas. *Approximation of large-scale dynamical systems*, volume 6. SIAM, 2005.
- [4] C. Ballew and T. Trogdon. <https://github.com/cade-b/RecurrenceCoefficients.jl>, 2023.
- [5] C. Ballew and T. Trogdon. The Akhiezer iteration. *arXiv preprint 2312.02384*, 2023.
- [6] C. Ballew and T. Trogdon. A Riemann–Hilbert approach to computing the inverse spectral map for measures supported on disjoint intervals. *Studies in Applied Mathematics*, 152(1):31–72, 2024.
- [7] C. Ballew, T. Trogdon, and H. Wilber. <https://github.com/cade-b/AkhiezerSylvester>, 2025.
- [8] J. Banks, J. Garza-Vargas, A. Kulkarni, and N. Srivastava. Pseudospectral Shattering, the Sign Function, and Diagonalization in Nearly Matrix Multiplication Time. *Foundations of Computational Mathematics*, 23(6):1959–2047, 2022.
- [9] R. H. Bartels and G. W. Stewart. Algorithm 432 [C2]: Solution of the matrix equation  $AX + XB = C$  [F4]. *Commun. ACM*, 15(9):820–826, 1972.
- [10] B. Beckermann. An error analysis for rational Galerkin projection applied to the Sylvester equation. *SIAM Journal on Numerical Analysis*, 49(6):2430–2450, 2011.

- [11] B. Beckermann, A. Cortinovis, D. Kressner, and M. Schweitzer. Low-rank updates of matrix functions II: Rational Krylov methods. *SIAM Journal on Numerical Analysis*, 59(3):1325–1347, 2021.
- [12] B. Beckermann and A. Townsend. Bounds on the singular values of matrices with displacement structure. *SIAM Review*, 61(2):319–344, 2019.
- [13] P. Benner. Solving large-scale control problems. *IEEE Control Systems Magazine*, 24(1):44–59, 2004.
- [14] P. Benner, R.-C. Li, and N. Truhar. On the ADI method for Sylvester equations. *Journal of Computational and Applied Mathematics*, 233(4):1035–1045, 2009.
- [15] P. Benner, R.-C. Li, and N. Truhar. On the ADI method for Sylvester equations. *Journal of Computational and Applied Mathematics*, 233(4):1035–1045, 2009.
- [16] P. Benner and E. S. Quintana-Ortí. Solving stable generalized Lyapunov equations with the matrix sign function. *Numerical Algorithms*, 20(1):75–100, 1999.
- [17] M. Berljafa and S. Guttel. The RKFIT algorithm for nonlinear rational approximation. *SIAM Journal on Scientific Computing*, 39(5):A2049–A2071, 2017.
- [18] D. A. Bini, B. Iannazzo, and B. Meini. *Numerical Solution of Algebraic Riccati Equations*. Society for Industrial and Applied Mathematics, 2011.
- [19] N. Boullé and A. Townsend. Computing with Functions in the Ball. *SIAM Journal on Scientific Computing*, 42(4):C169–C191, 2020.
- [20] S. Brahma and B. Datta. An optimization approach for minimum norm and robust partial quadratic eigenvalue assignment problems for vibrating structures. *Journal of Sound and Vibration*, 324(3-5):471–489, 2009.
- [21] D. Calvetti and L. Reichel. Application of ADI iterative methods to the restoration of noisy images. *SIAM Journal on Matrix Analysis and Applications*, 17(1):165–186, 1996.
- [22] Y. Chen and A. R. Its. A Riemann–Hilbert approach to the Akhiezer polynomials. *Philosophical Transactions of the Royal Society A: Mathematical, Physical and Engineering Sciences*, 366(1867):973–1003, mar 2008.
- [23] E. D. Denman and A. N. Beavers, Jr. The matrix sign function and computations in systems. *Applied mathematics and Computation*, 2(1):63–94, 1976.
- [24] V. Druskin, L. Knizhnerman, and V. Simoncini. Analysis of the rational Krylov subspace and ADI methods for solving the Lyapunov equation. *SIAM Journal on Matrix Analysis and Applications*, 49(5):1875–1898, 2011.
- [25] D. Fortunato and A. Townsend. Fast Poisson solvers for spectral methods. *IMA Journal of Numerical Analysis*, 40(3):1994–2018, 2020.
- [26] Z. Gajic and M. T. J. Qureshi. *Lyapunov matrix equation in system stability and control*. Courier Corporation, 2008.
- [27] W. Gautschi. *Orthogonal Polynomials: Computation and Approximation*. Oxford University Press, 2004.
- [28] E. S. Gawlik and M. Leok. Iterative Computation of the Fréchet Derivative of the Polar Decomposition. *SIAM Journal on Matrix Analysis and Applications*, 38(4):1354–1379, 2017.
- [29] W. B. Gragg and W. J. Harrod. The numerically stable reconstruction of Jacobi matrices from spectral data. *Numerische Mathematik*, 44(3):317–335, 1984.
- [30] S. Gugercin, D. C. Sorensen, and A. C. Antoulas. A modified low-rank Smith method for large-scale Lyapunov equations. *Numerical Algorithms*, 32(1):27–55, 2003.
- [31] N. J. Higham. *Functions of matrices: theory and computation*. SIAM, 2008.
- [32] N. J. Higham and S. D. Relton. Higher Order Fréchet Derivatives of Matrix Functions and the Level-2 Condition Number. *SIAM Journal on Matrix Analysis and Applications*, 35(3):1019–1037, 2014.
- [33] A. Horning and A. Townsend. FEAST for Differential Eigenvalue Problems. *SIAM Journal on Numerical Analysis*, 58(2):1239–1262, 2020.
- [34] C. Kenney and A. J. Laub. Polar Decomposition and Matrix Sign Function Condition Estimates. *SIAM Journal on Scientific and Statistical Computing*, 12(3):488–504, 1991.
- [35] D. Kressner, S. Massei, and L. Robol. Low-rank updates and a divide-and-conquer method for linear matrix equations. *SIAM Journal on Scientific Computing*, 41(2):A848–A876, 2019.
- [36] A. Laub. Numerical linear algebra aspects of control design computations. *IEEE transactions on automatic control*, 30(2):97–108, 1985.
- [37] J.-R. Li and J. White. Low rank solution of Lyapunov equations. *SIAM Journal on Matrix Analysis and Applications*, 24(1):260–280, 2002.
- [38] T. A. Manteuffel. The Tchebychev iteration for nonsymmetric linear systems. *Numerische Mathematik*, 28(3):307–327, 1977.
- [39] T. A. Manteuffel. Adaptive procedure for estimating parameters for the nonsymmetric Tchebychev iteration. *Numerische Mathematik*, 31(2):183–208, June 1978.
- [40] S. Massei, M. Mazza, and L. Robol. Fast solvers for two-dimensional fractional diffusion equations using rank structured matrices. *SIAM Journal on Scientific Computing*, 41(4):A2627–A2656, 2019.
- [41] R. Mathias. A Chain Rule for Matrix Functions and Applications. *SIAM Journal on Matrix Analysis and Applications*, 17(3):610–620, 1996.

- [42] Y. Nakatsukasa, Z. Bai, and F. Gygi. Optimizing Halley’s iteration for computing the matrix polar decomposition. *SIAM Journal on Matrix Analysis and Applications*, 31(5):2700–2720, 2010.
- [43] Y. Nakatsukasa and R. W Freund. Computing fundamental matrix decompositions accurately via the matrix sign function in two iterations: The power of Zolotarev’s functions. *SIAM Review*, 58(3):461–493, 2016.
- [44] S. Olver, R. M. Slevinsky, and A. Townsend. Fast algorithms using orthogonal polynomials. *Acta Numerica*, 29:573–699, 2020.
- [45] S Olver and A Townsend. A Fast and Well-Conditioned Spectral Method. *SIAM Review*, 55(3):462–489, jan 2013.
- [46] D. Palitta, M. Schweitzer, and V. Simoncini. Sketched and truncated polynomial Krylov subspace methods: Matrix Sylvester equations. *Mathematics of Computation*, 2024.
- [47] I. P. A. Papadopoulos, T. S. Gutleb, R. M. Slevinsky, and S. Olver. Building Hierarchies of Semiclassical Jacobi Polynomials for Spectral Methods in Annuli. *SIAM Journal on Scientific Computing*, 46(6):A3448–A3476, 2024.
- [48] T. Penzl. A cyclic low-rank Smith method for large sparse Lyapunov equations. *SIAM Journal on Scientific Computing*, 21(4):1401–1418, 1999.
- [49] J. D. Roberts. Linear model reduction and solution of the algebraic Riccati equation by use of the sign function. *International Journal of Control*, 32(4):677–687, 1980.
- [50] A. Ruhe. Rational Krylov sequence methods for eigenvalue computation. *Linear Algebra and its Applications*, 58:391–405, 1984.
- [51] J. Sabino. *Solution of large-scale Lyapunov equations via the block modified Smith method*. PhD thesis, Rice University, 2007.
- [52] V. Simoncini. A new iterative method for solving large-scale Lyapunov matrix equations. *SIAM Journal on Scientific Computing*, 29(3):1268–1288, 2007.
- [53] V. Simoncini. Computational methods for linear matrix equations. *SIAM Review*, 58(3):377–441, 2016.
- [54] J. Słomka, A. Townsend, and J. Dunkel. Stokes’ second problem and reduction of inertia in active fluids. *Physical Review, Fluids*, 3(10):103304, 2018.
- [55] R. A. Smith. Matrix Equation  $XA+BX=C$ . *SIAM Journal on Applied Mathematics*, 16(1):198–201, 1968.
- [56] G. Szegő. *Orthogonal Polynomials*, volume 23 of *Colloquium Publications*. American Mathematical Society, Providence, Rhode Island, 1939.
- [57] L. N. Trefethen and J. A. C. Weideman. The Exponentially Convergent Trapezoidal Rule. *SIAM Review*, 56(3):385–458, 2014.
- [58] L. N. Trefethen and H. D. Wilber. Computation of Zolotarev rational functions. *arXiv preprint arXiv:2408.14092*, 2024.
- [59] T Trogdon. The ultraspherical rectangular collocation method and its convergence. *arXiv preprint 2401.03608*, 2024.
- [60] P. M. Van Dooren. Structured linear algebra problems in digital signal processing. In *Numerical linear algebra, digital signal processing and parallel algorithms*, pages 361–384. Springer, 1991.
- [61] J. C. Wheeler. Modified moments and continued fraction coefficients for the diatomic linear chain. *The Journal of Chemical Physics*, 80(1):472–476, 1984.

UNIVERSITY OF WASHINGTON, SEATTLE, WA  
 Email address: `ballew@uw.edu`

UNIVERSITY OF WASHINGTON, SEATTLE, WA  
 Email address: `trogdon@uw.edu`

UNIVERSITY OF WASHINGTON, SEATTLE, WA  
 Email address: `hdw27@uw.edu`